

**MASTER**

**A Laser Cutting tool for Laryngeal Surgery**

van de Ven, T.A.J.M.

*Award date:*  
2011

[Link to publication](#)

**Disclaimer**

This document contains a student thesis (bachelor's or master's), as authored by a student at Eindhoven University of Technology. Student theses are made available in the TU/e repository upon obtaining the required degree. The grade received is not published on the document as presented in the repository. The required complexity or quality of research of student theses may vary by program, and the required minimum study period may vary in duration.

**General rights**

Copyright and moral rights for the publications made accessible in the public portal are retained by the authors and/or other copyright owners and it is a condition of accessing publications that users recognise and abide by the legal requirements associated with these rights.

- Users may download and print one copy of any publication from the public portal for the purpose of private study or research.
- You may not further distribute the material or use it for any profit-making activity or commercial gain

T.A.J.M. van de Ven  
Juni 2011

# A Laser Cutting Tool for Laryngeal Surgery

T.A.J.M. van de Ven

CST 2011.046

Master's thesis

Coach(es): dr.ir. P.C.J.N. Rosielle, prof.dr B. Kremer

Supervisor: prof.dr.ir. M. Steinbuch

Eindhoven University of Technology  
Department of Mechanical Engineering  
Control Systems Technology

Eindhoven, June, 2011

### **Abstract**

Cancer is the number one cause of death in the Netherlands. A lot of research is being conducted to the treatment of cancer. To also contribute to this research this report is focused on the design of a laser cutting tool for laryngeal surgery. Laryngeal surgery is mostly done minimally invasive. This is done by inserting a tube (laryngoscope) via the mouth and throat to the larynx. This way of operating is limiting the freedom of the tool and cutting laser because the tube/throat is limiting all the movements of the tool, except the rotation around and translation along the centerline of the tube. The laser tool designed uses mirrors to cut under an angle with respect to the centerline of the laryngoscope. This makes it possible to cut underneath the tumor such that more healthy tissue can be left behind such that the risk of complications such as loss or change of voice is reduced.

# Contents

<b>1</b>	<b>Introduction</b>	<b>1</b>
<b>2</b>	<b>Laryngeal Surgery</b>	<b>3</b>
2.1	Introduction . . . . .	3
2.2	Surgical Procedure . . . . .	4
2.3	Assumptions and Criteria . . . . .	9
<b>3</b>	<b>Frame</b>	<b>11</b>
3.1	Introduction . . . . .	11
3.2	Rail Clamps . . . . .	11
3.3	Frame Tube . . . . .	13
3.4	Laryngoscope Arm . . . . .	14
3.5	Support Rods . . . . .	16
<b>4</b>	<b>Laser Tool</b>	<b>19</b>
4.1	Introduction . . . . .	19
4.2	$x, y, \theta$ -Manipulator . . . . .	20
4.2.1	Concept . . . . .	20
4.2.2	$x, y, \theta$ -Mechanism . . . . .	21
4.3	$z$ -Manipulator . . . . .	23
4.3.1	Concept . . . . .	23
4.3.2	Mechanism . . . . .	26
4.3.3	Actuation . . . . .	28
4.4	Cutting Tool . . . . .	31

4.4.1	Concept . . . . .	31
4.4.2	Cutting Tool Tip Mechanism . . . . .	32
4.4.3	Actuation . . . . .	39
<b>5</b>	<b>Conclusion</b>	<b>45</b>
	<b>Bibliography</b>	<b>47</b>
<b>A</b>	<b>z-Manipulator</b>	<b>49</b>
<b>B</b>	<b>Cutting Tool</b>	<b>51</b>
<b>C</b>	<b>Forceps</b>	<b>53</b>

# Chapter 1

## Introduction

Cancer is the number one cause of death in the Netherlands. In 2009 31.6% of the people deceased died of cancer, heart and vascular system diseases come second with 29.0%. Because cancer is death cause number one, a lot research is done to the treatment of cancer. There are different kinds of cancer some are more common than other.

To contribute to the research of the treatment of cancer this report is focused on designing a laser cutting tool for laryngeal surgery. Because of all the people died of cancer 2.7% of the men and 1.5% of the woman died of laryngeal cancer. Figure 1.1 shows on the right healthy vocal folds and on the left vocal fold with cancer as an example. This is the view a surgeon has through a laryngoscope. Which is a tube inserted via the mouth in the throat of the patient for access to the larynx via the mouth.

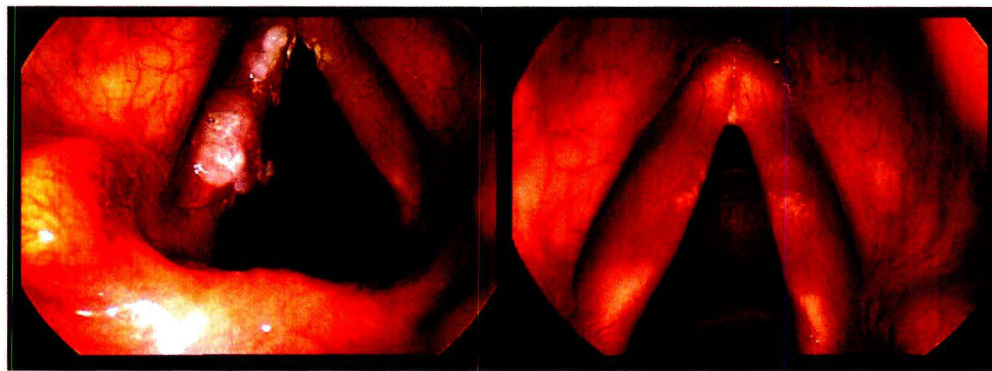


**Figure 1.1:** A surgeons view on the vocal folds with on the right healthy vocal folds and on the left vocal folds with cancer

From conversations with an ENT surgeon and literature [1] it can be concluded that there is a need for tools that have more freedom off the centerline of the throat. Such that the tools can work under an adjustable angle. The current method is changing tools when it is necessary to work under an other angle. This freedom is wanted in the tool itself. Most of the time laryngeal surgery is done minimally invasive. Minimally invasive means that the surgery is done with minimum damage to healthy tissue as possible. Therefore laryngeal surgery is often done via a laryngoscope which is inserted in the throat. Such that it is not necessary to cut someone's throat open and therefore outside scarring and recovery time is brought to a minimum.

This way of operating is limiting the freedom of the tools because the tube/throat is limiting all the movements of the tools, except the rotation around the centerline of the tube and translation along this center line. Because of that the current laser tool can only cut on the plane perpendicular to the centerline

of the laryngoscope (transverse plane). So when a tumor needs to be removed they have to cut through the entire vocal fold. An other possibility is to use a pair of forceps to manipulate the tumor such that you can cut underneath it. This manipulation is limited because extreme manipulation such as bending can damage the vocal folds.

To overcome these problems a laser tool is designed. This laser tool makes it possible to cut underneath the tumor. When cutting underneath the tumor less healthy tissue is damaged/removed during surgery. If more healthy tissue is left in place the risk of loss or change of voice is lower. The principle of the cutting tool is grabbing the tumor with a suction tube, next to this suction tube is a laser cutting tool which cuts a half circle around the tumor. With an adjustable mirror the laser can be gradually aimed under the tumor to cut around the tumor instead of cutting through the entire vocal fold. So instead of manipulating the tumor or vocal fold to cut underneath the tumor the laser beam is manipulated. Also the manipulators for positioning the entire laser tool on the tumor are designed.

In chapter 2 the surgical procedure of removing a tumor or polyp from the vocal folds is discussed. Chapter 2 also gives criteria and assumptions that are needed to come to a design. In chapter 3 the design of the tool frame is discussed. This chapter contains the design of the clamps and the main frame tube to which the laryngoscope and the laser tool can be connected. The parts connected to this frame tube are the laryngoscope arm and the support rods. The laryngoscope arm is used to fix the laryngoscope in place and the support rods are used to fix the laser tool to the frame. In chapter 4 the actual laser tool is discussed, in section 4.2 and 4.3 the  $x,y,\theta$ -manipulator and  $z$ -manipulator are discussed. These manipulators are used to position the tip of the laser tool on the tumor. Then the cutting tool is discussed in section 4.4. In this section the tool and its actuation are discussed

## Chapter 2

# Laryngeal Surgery

### 2.1 Introduction

In this chapter the complete surgical procedure of laryngeal surgery is explained step by step. Figure 2.1 presents an anatomical chart of the human head with the larynx. In this report laryngeal surgery means in particular the removal of a tumor or polyp from the Vestibular folds (false vocal folds) or the vocal folds (true vocal folds). In figure 2.2 an anatomical chart of the larynx is shown with the (vestibular) vocal folds pointed out. This chapter will also point out the difficulties encountered during laryngeal surgery and which of these difficulties were selected to overcome with the design of new tools.

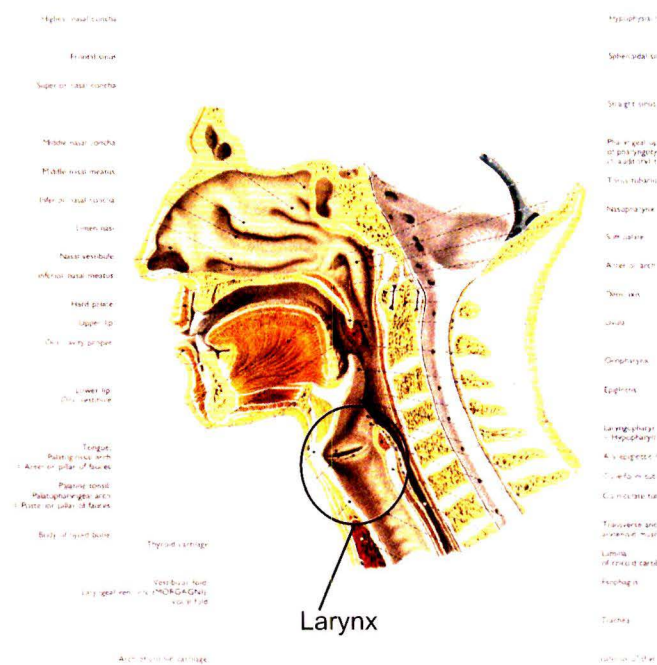


Figure 2.1: Anatomy of the human head and neck [2]



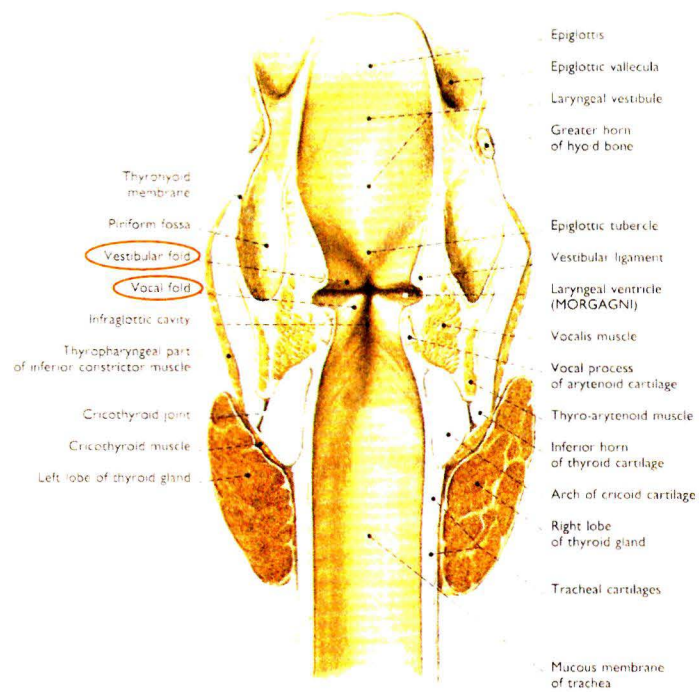


Figure 2.2: Anatomy of the larynx [2]

## 2.2 Surgical Procedure

First an overview of the layout of the operating room is shown in figure 2.3. In this figure it becomes clear that one side of the table is taken by all the anesthetic appliances such as artificial respiration and drug supplies which are operated by one or two anesthesiologists. The surgeon is sitting at the head side of the operating table. Next to the surgeon is the assistant who is handing over all the tools and medical supplies such as medical gauze.

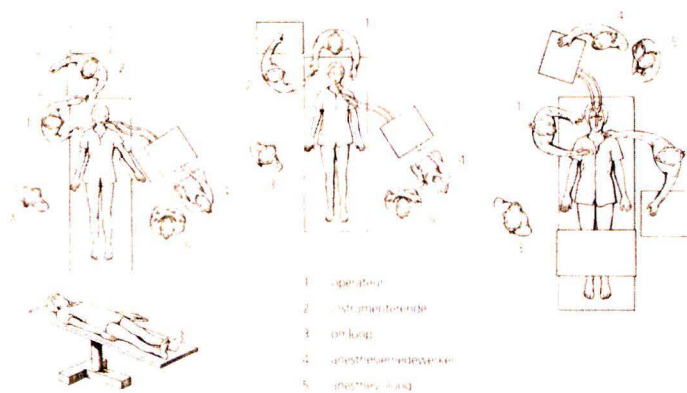
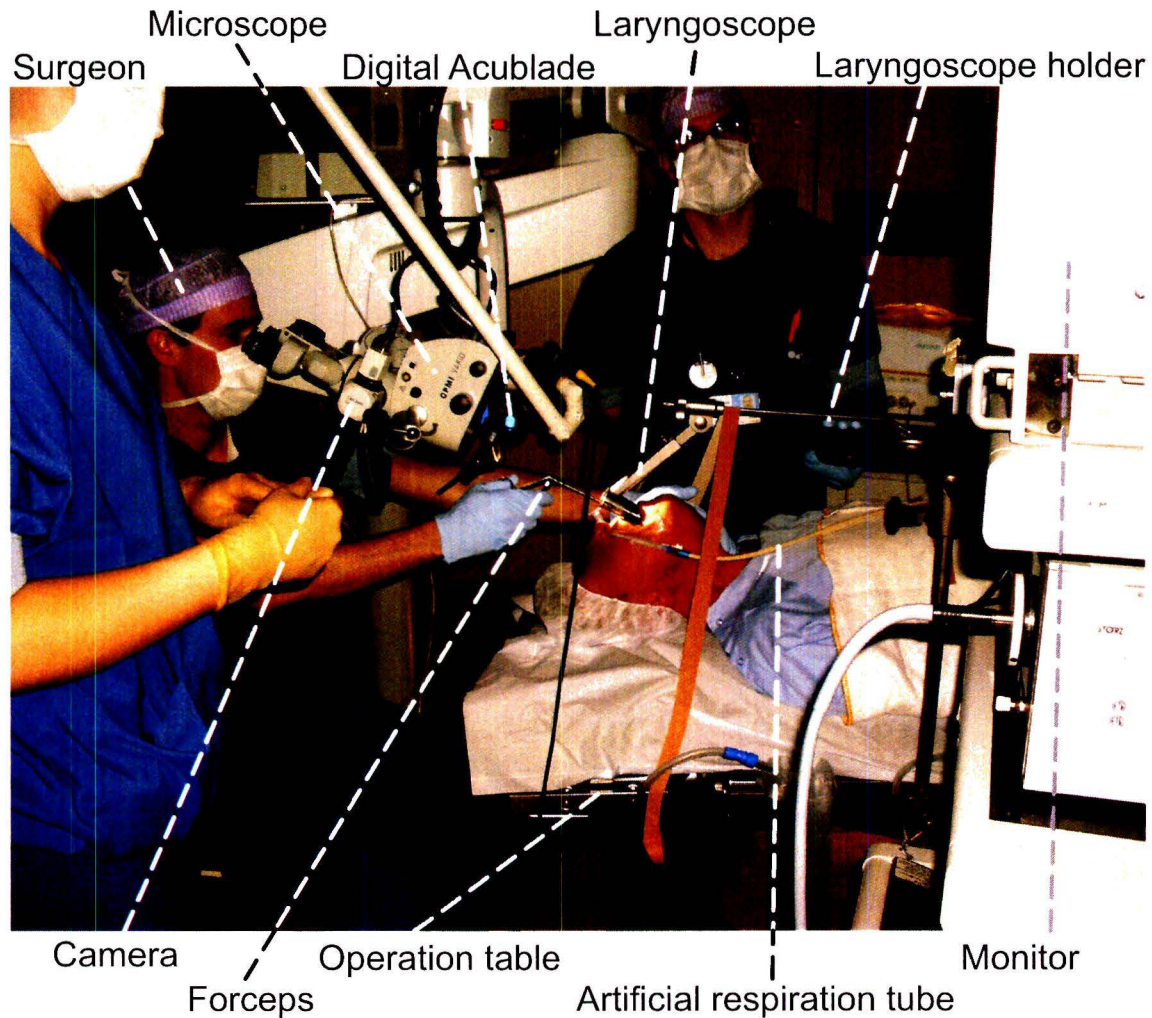


Figure 2.3: Topview of the most common floorplans of the operating room during laryngeal surgery [3]

Figure 2.4 shows how the patient is lying on the operating table and how the surgeon is sitting with respect to the patient. It also shows how all the instruments and tools used are positioned. The surgeon is sitting far from the patients head this forces the surgeon to work with his arms stretched. Nothing is supporting the surgeons hands and arms this posture can be very tiring during long operations and makes it hard to hold the tools steady.



**Figure 2.4:** *Position of the surgeon, patient and instruments*

Now the surgical procedure is explained in chronological order. First, a small tube for artificial respiration is inserted via the nose the tube is pointed out in figure 2.4. This is not the common type of artificial respiration normally a big tube is inserted via the mouth to the lungs with an air flow similar with the normal air flow of the lungs. In this case the small tube is used because the mouth, throat and airway have to stay clear for access to the larynx. This small tube is not capable to create an airflow similar to the normal airflow to the lungs. Therefore high frequent and high pressure pulses of oxygen are going through this small tube. To make sure that enough oxygen reaches the lungs.

Next a tube called a laryngoscope is inserted via the mouth. Figure 2.5 shows a standard laryngoscope as can be found in the Storz catalog [4] and figure 2.4 shows how the laryngoscope is positioned in a humans throat. The laryngoscope lines the mouth, throat and larynx up and provides protection for the surrounding tissue from the tools. Through the laryngoscope the surgeon can reach to the larynx with his tools. After the insertion of the laryngoscope a kind of gel donut (figure 2.6) is put under the head of the patient such that the head stays in place during surgery

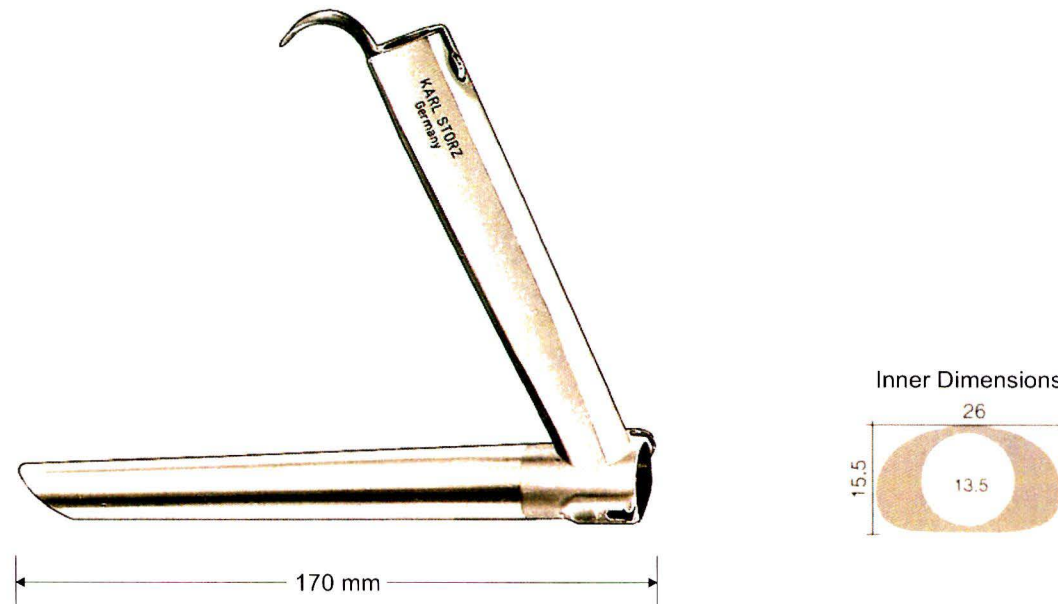


**Figure 2.5:** A standard medium laryngoscope [4]



**Figure 2.6:** Gel donut to keep the patients head in place

The next step is to place the microscope, with the laser module attached, in front of the laryngoscope. In figure 2.4 the position of the microscope with respect to the laryngoscope can be seen. This figure also shows the camera which is putting the view of the microscope on a screen. This is done such that the other persons in the operating room can see what the surgeon is doing.

The surgeon in figure 2.4 is holding a pair of forceps, figure 2.7 shows some of the most commonly used cutting- and grasping forceps. In this picture it can be seen that the distance between the scissor like handles and the tool head is  $230\text{mm}$ . This length of the tool is needed to reach the larynx through the laryngoscope. The tools shown in figure 2.7 are mainly used for biopsy and manipulating the tissue. To remove tumors and polyps mostly a laser is used.

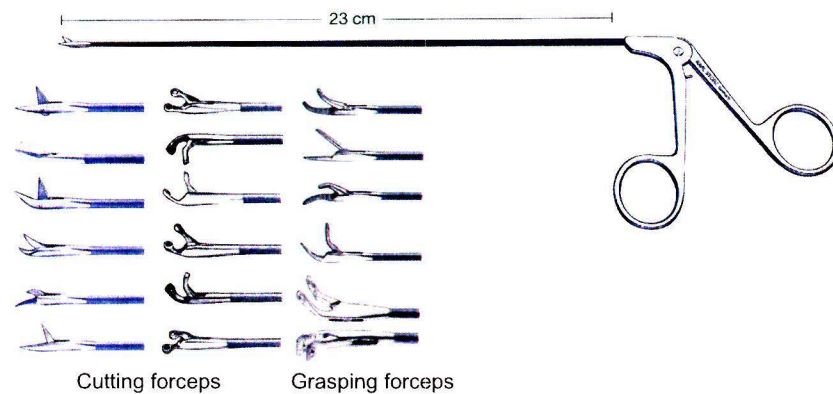


**Figure 2.7:** A standard pair of forceps (top) with different kind of tooltips (bottom) [4]

For the purpose of removing tumors a special laser is developed by Lumenis Surgical. The laser is a separate module which can be used for several kinds of surgery when using different kind of attachments. Figure 2.8 shows this laser, it is called the AcuPulse™ [5]. It is a CO<sub>2</sub> laser, the advantage of using a CO<sub>2</sub> laser is that the light emitted is in the infrared spectrum (wavelength =  $10.6\mu\text{m}$ ). Water absorbs this light very well, since the human body consists of water for 60 % this will be a good cutting laser. The attachment used for laryngeal surgery is the Digital AcuBlade™ [6] which is shown in figure 2.9.



**Figure 2.8:** AcuPulse™ CO<sub>2</sub> with display

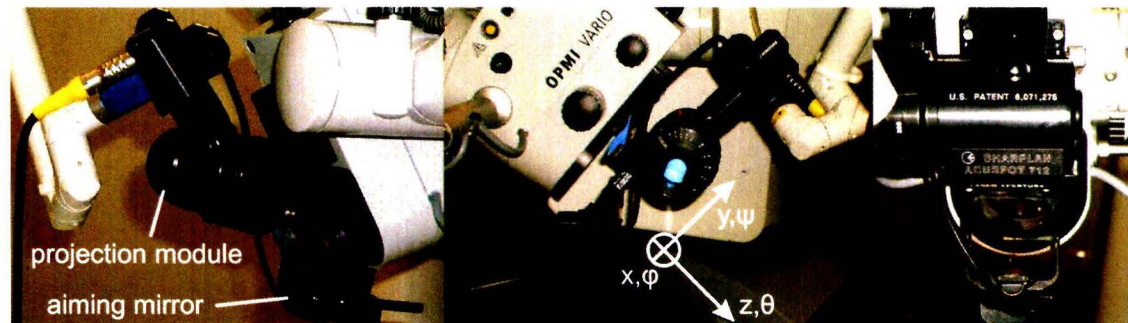


Figure 2.9: 3D, sideview and frontview of the Digital AcuBlade™

The module consists of two parts. The first part is the projection module and the second is the aiming mirror. In the projection module different shapes which are shown in figure 2.10 are created. These projections are made with two mirrors both with only one DOF, one with  $\psi$  and one with  $\phi$ . In theory all shapes in the  $x,y$ -plane can be made with those two DOF's but only the shapes from figure 2.10 are implemented in the software of the module. The shape wanted can be chosen on the display of the AcuPulse™. The AcuPulse™ has a user friendly interface. On the touchscreen the shape, incision width and length and the incision depth can be chosen. The laser module will then do all the calculations to make the projection and use the correct amount of power to reach the right incision depth.

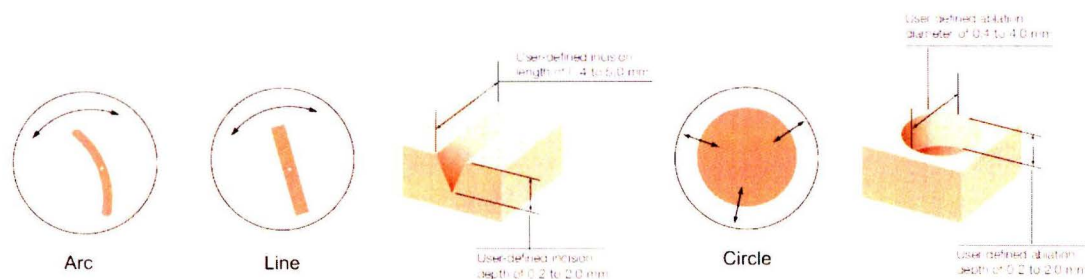
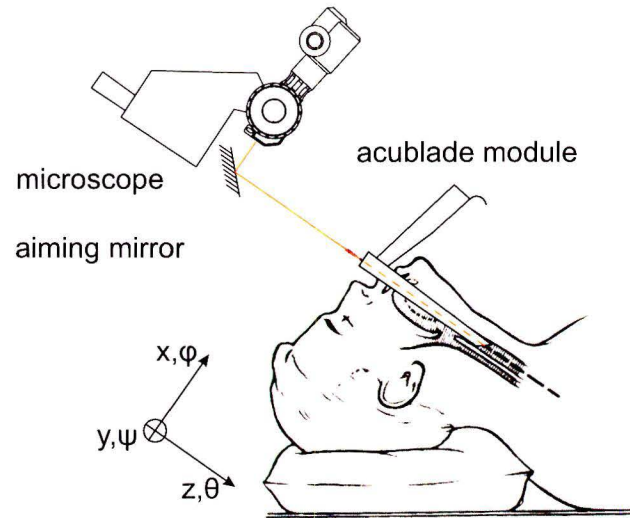


Figure 2.10: Different projections that are possible with the AcuBlade™ [6]

Now the selected laser beam shape comes out of the projection module onto the aiming mirror. This aiming mirror is used to manipulate the laser beam. The setup is schematically presented in figure 2.11. This aiming mirror can be manipulated with a joystick. This joystick has three DOF's  $\phi$ ,  $\psi$  and  $\theta$ . The  $\theta$  is rotation around the centerline of the laryngoscope, this rotation is made digitally with the projection module. The  $\phi$  and  $\psi$  rotations are transferred from the joystick to the aiming mirror. This  $\phi$  and  $\psi$  rotation result in an adjustment in the  $x,y$ -plane down the laryngoscope.

When the laser beam is aimed correctly the surgeon can fire a shot with the laser. Each shot will cut progressively deeper into the tissue. When shots are fired at different places the desired shape of the cut can be made. When enough shots are fired the piece of tissue will come loose.

The difficulties encountered with laryngeal surgery have mostly to do with the laryngoscope. This laryngoscope limits the freedom of the tools because it is a tube. The only directions a tube will not limit are the movement along the centerline of the tube and the rotations around it. Therefore the laser can only cut on the transverse plane which is the plane perpendicular to the centerline of the laryngoscope. Therefore the goal of this study is to design a laser tool with more freedom than the current laser.



**Figure 2.11:** Schematic representation of the position of the AcuBlade™ with respect to the patient

### 2.3 Assumptions and Criteria

To design the tools for the ENT-surgeon some assumptions have to be made. These assumptions and data collected are presented in this section. All people are different which result in many different types of laryngoscopes that are available for laryngeal surgery. Mostly the one used is determined by the size of the patient and the surgeon's experience. For this design the medium laryngoscope (type KLEINSASSER 8590 C [4]) shown in figure 2.5 is chosen. This choice is made because this laryngoscope will fit most patients. This gives the range of the tool in the  $x, y$  (transverse)-plane which is perpendicular to the laryngoscope centerline. This range is 0 to 13mm for  $x$  and  $y$  since the diameter of the laryngoscope opening is 13mm.

When an object is placed in front of the laryngoscope it may not limit the movements of the forceps. Therefore the object placed in front of the laryngoscope may not be thicker than 50mm because the forceps have a length of 230mm and the laryngoscope has a length of 170mm. When something is placed in front of the laryngoscope of 50mm thick there is still 10mm left for the manipulation of the forceps. Also the size of the hole that has to be in the object that is placed in front of the laryngoscope has restrictions. The size of the hole is determined by the maximum angle the forceps can reach with respect to the laryngoscope centerline. In figure 2.12 the hole diameter is given as function of the thickness of the object placed in front of the laryngoscope.

The most common tumors are approximately 1mm in diameter. The margin around the tumor when it is cut is approximately 1 – 2mm. So at least 1 or 2mm healthy tissue has to be cut away to be sure the tumor and all the damaged tissue is removed. Due to the size of the average tumor the cross-section of the cutting laser beam is assumed to be max  $0.4 \times 1mm$ . 0.4mm is the minimal cutting width of the laser beam and a cutting length of 1mm should be sufficient for this size tumors.

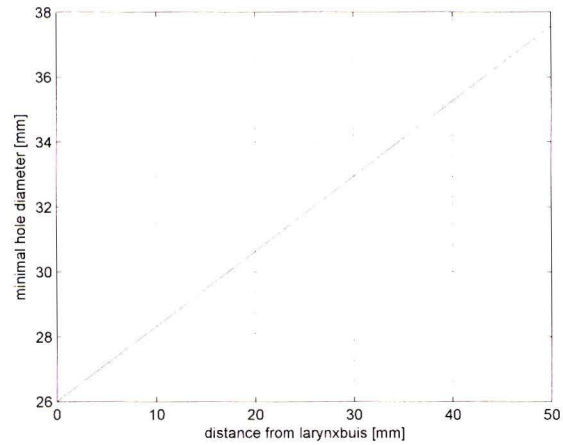


**Figure 2.12:** Minimum hole diameter of the body which can be placed in front of the laryngoscope

Figure 2.13 shows the dimension of the human head which is important for this design. The chin-crown distance has a minimal value of  $166\text{mm}$  and a maximum of  $230\text{mm}$  the average is  $198\text{mm}$  [7]. This determines the range of the height adjustment for the laryngoscope fixing. The range of this height adjustment has to be at least  $64\text{mm}$ .

The table size is determining for the frame width. From research done the bed width appeared to be in the range from  $480\text{mm}$  to  $690\text{mm}$ . This bed of  $690\text{mm}$  is a peak the average will lay about a width of  $520\text{mm}$ . Which is the assumed bed width for this design.

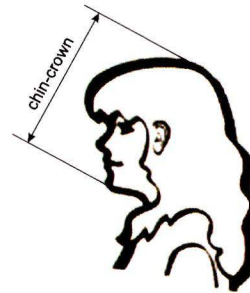


**Figure 2.13:** Definition of the chin-crown distance of the human head [7]

## Chapter 3

# Frame

### 3.1 Introduction

The lasertool and laryngoscope have to be fixed to the world (operating table). For that purpose a frame is designed. The frame consists of two clamps to fix the frame to the operating table. These clamps are discussed in section 3.2. In section 3.3 the tube of the frame which is connecting the two clamps will be shown. The frame tube is used to attach the laryngoscope arm (section 3.4) and the support rods (section 3.5). The laryngoscope arm is used to fix the laryngoscope during surgery and the support rods are used to fix the lasertool to the frame.

### 3.2 Rail Clamps

The goal of these clamps is to fix the frame to the operating table. It should be easy to undo the clamps to make small adjustments along the table rail. It should also be possible to place the frame on the table rails from above. Such that it is not necessary to slide the frame over the table rails from one of the intermediate rail ends. This makes it easier to place the frame on the table and reduces the risk to hit the patient with the frame. In figure 3.1 an overview of the frame attached to the operating table is shown. The clamps are attached to both ends of the frame tube.

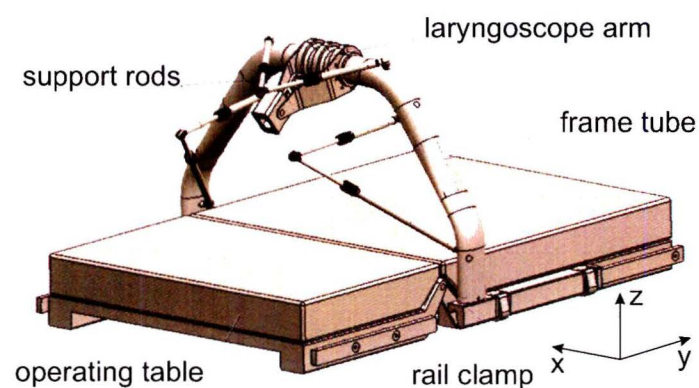


**Figure 3.1:** Overview of the frame for the laser tool and laryngoscope



The choice of using two clamps on two rails instead of one clamp on one rail is made because it has to fix the laryngoscope and the lasertool in the approximate middle of the operating table. Using one clamp will result in a moment on the rail, this is schematically represented in figure 3.2. In this figure  $F_z$  represents the gravitational force of the laryngoscope and the laser tool. In this figure also the case with two clamps is shown. The rectangular cross section of the table rail makes it such that it has a low torsional stiffness compared to other shapes. The stiffness of the rail in different directions is given in figure 3.3. The advantage of using two clamps is that the moment on the table rail will disappear. When the clamps are on both sides of the operating table only a downward force will act on the rail (figure 3.2). This downward force is in this case only half of the gravitational force because there are two clamps. Therefore the load per rail is smaller. An other advantage is that this downward force is acting in the most stiff direction of the rail.

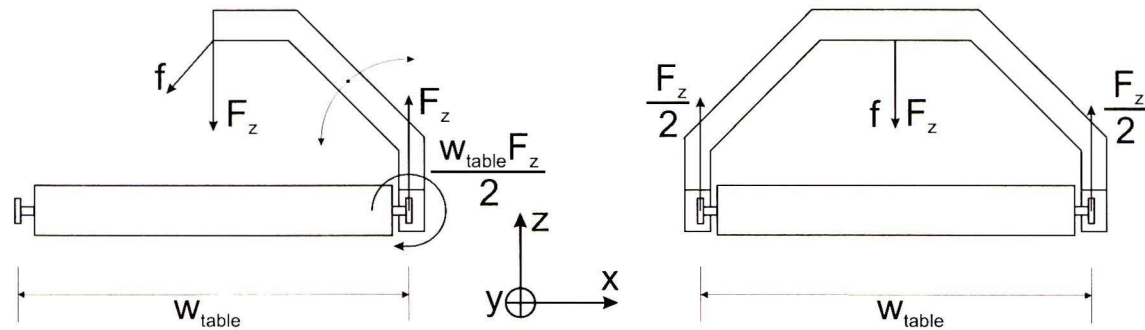


**Figure 3.2:** Forces acting on the operating table rail when using one clamp (left) or two clamps (right)

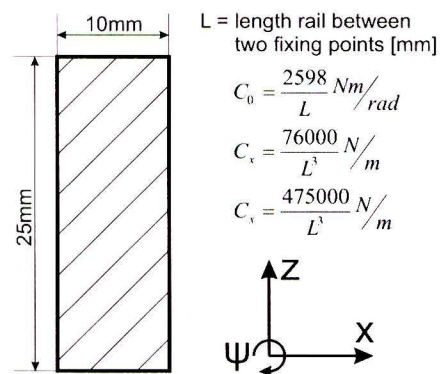


**Figure 3.3:** Cross section of the rail attached to the operating table

The body of the clamp is made such that it spans at least two mounting points of the rail. Mounting points are the places where the rail is attached to the frame of the operating table. The reason for over-spanning two mounting points is because these points are the most rigid points of the rail. These points are reasonably far apart which makes the clamp very long and therefore makes the frame better resistant for tipping over (makes it stiff in the  $\phi$ -direction).

The clamp mechanism in open and closed situation is shown in figure 3.4. In this figure the body of the clamp is made translucent in the side view. The clamp consists of three parts, the clamp body which is resting on top of the rail, the clamp swing arm which has a pivot point on the body (pivot 1) and the clamp arm which has a pivot point on the swing arm (pivot 2). The clamp is made such that it is bistable. When pivot 2 is left of pivot 1 the clamp is locked when it is at the right of pivot 1 the clamp is open. When pivot 2 is at the left of pivot 1 the clamp stays locked because it is over the dead point of the clamp swing arm. Figure 3.4 also shows that when the clamp is in open position nothing is under the rail. This makes it possible to place the frame on the table from above and it can be taken off the same way.

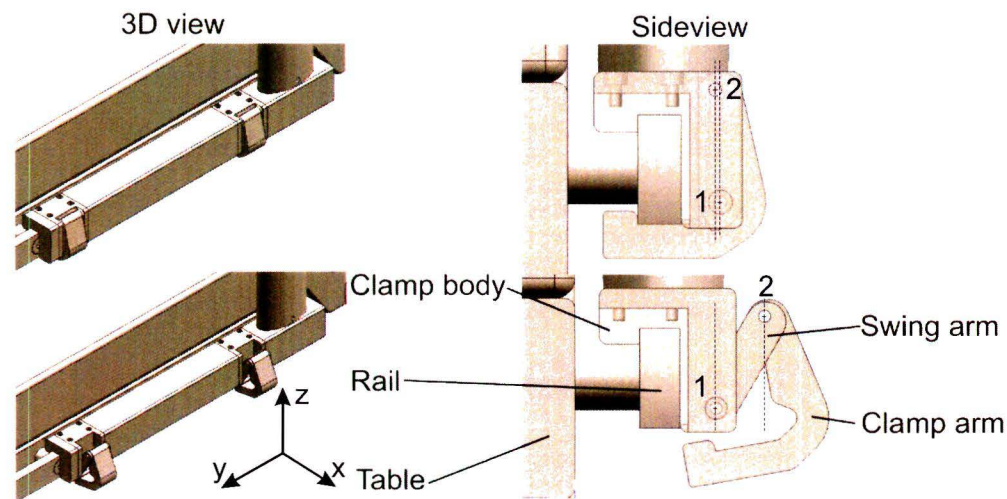


Figure 3.4: 3D and sideview of the rail clamp in closed (top) and open (bottom) position

### 3.3 Frame Tube

The frame tube is used to mount the laryngoscope and the laser tool. The tube is made as a portal such that the ends are supported by the two clamps. The reason why two clamps are used is explained in the previous section.

At the top of the portal, the tube has a straight section. This straight section is needed to give the arm to fix the laryngoscope some freedom in the x-direction (this is explained in section 3.4). Then the tube is bent down with two bends to the rail clamps. The ends of the tube are deformed to an elliptical shape. This will give the frame extra stiffness in the y and  $\psi$  direction at the point where they are attached to the clamps. Also the elliptical shape avoids that the clamps are unnecessarily wide.

In the tube six inserts are placed. The inserts are needed to fix ball joints to the frame. These ball joints will be used to fix the support rods, of the laser tool, to the frame. The locations of the inserts and the support rods will be explained in section 3.5. In figure 3.5 a schematic representation of how an insert is fixed in the tube is shown. A hole is drilled in the tube through both tube walls, then the insert is put through both holes in the tube wall [8]. Then the insert should be welded to the tube at both holes. This is done such that not only a small piece of the tube wall and its bending stiffness but the whole stiffness of the tube is used to keep the ball joint in place.

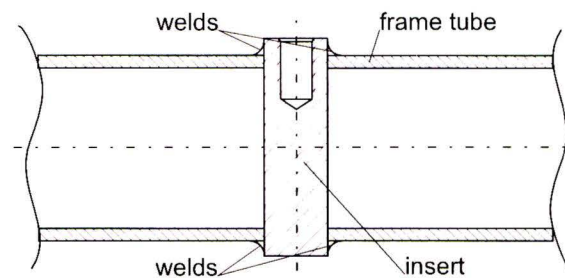


Figure 3.5: Schematic representation the insert fixation in the frame tube

### 3.4 Laryngoscope Arm

During this project the laryngoscope arm is not finished therefore in this section only the functions that should be present in the laryngoscope arm are explained. The current way of fixing is shown in figure 3.6. This is a very poor fixing because it is just one rod trying to fix six DOF but one rod can only fix one DOF therefore in this situation the laryngoscope is not fixed. This explains the need for an alternative.

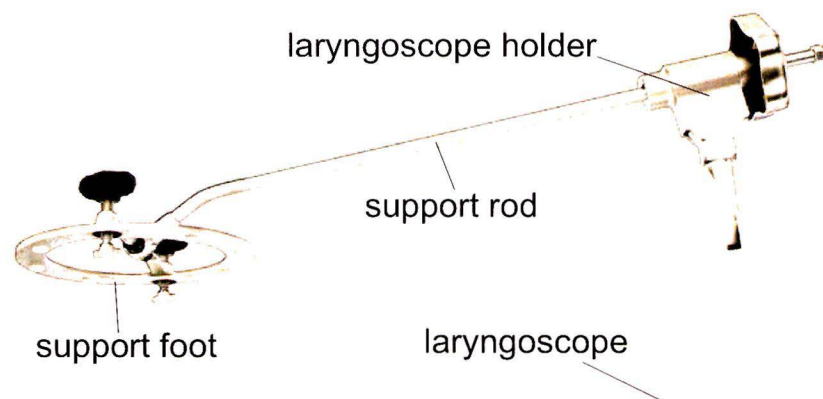


Figure 3.6: Current way of fixing a laryngoscope

The laryngoscope arm consist of three basic parts shown in figure 3.7. First the hub with which the laryngoscope arm is attached to the frame, the arm itself and the laryngoscope clamp. The hub gives the arm freedom in  $x$  and in  $\phi$ . This is shown in figure 3.8. The  $x$  freedom can be used when the patient is not laying exactly in the middle of the table. The  $\phi$  is used to adjust the height of the laryngoscope clamp. The  $x$  and  $\phi$  are locked by clamping the hub on the frame tube.

The laryngoscope clamp grasps the laryngoscope around the handle as close as possible to the tube of the laryngoscope. The laryngoscope has a pivot point which gives the laryngoscope clamp freedom in  $\phi$  direction. This is needed because the relative angle of the laryngoscope handle with respect to the laryngoscope arm is different for every patient because every patient has a different head-neck shape. The shape of the arm has to be designed such that it is as stiff as possible in all directions and makes good use of the stiffness of the frame tube.

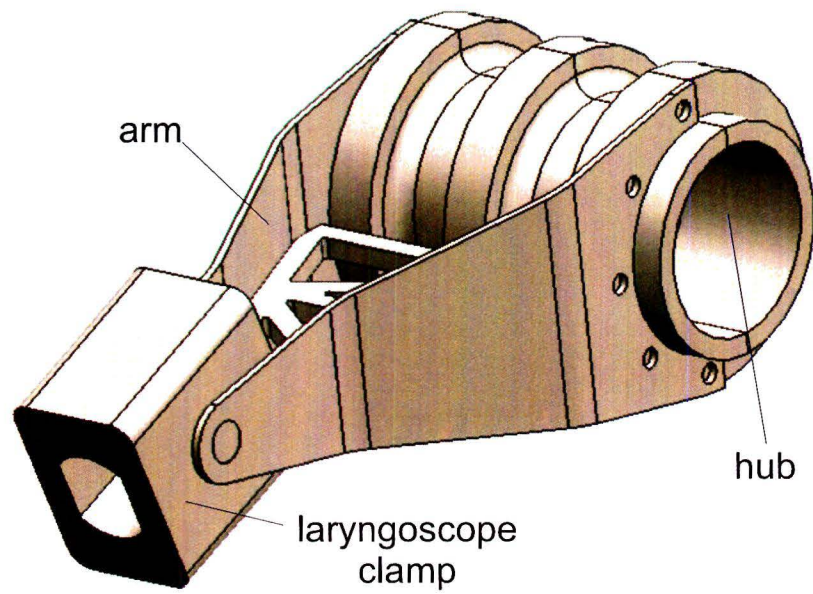


Figure 3.7: Laryngoscope arm overview

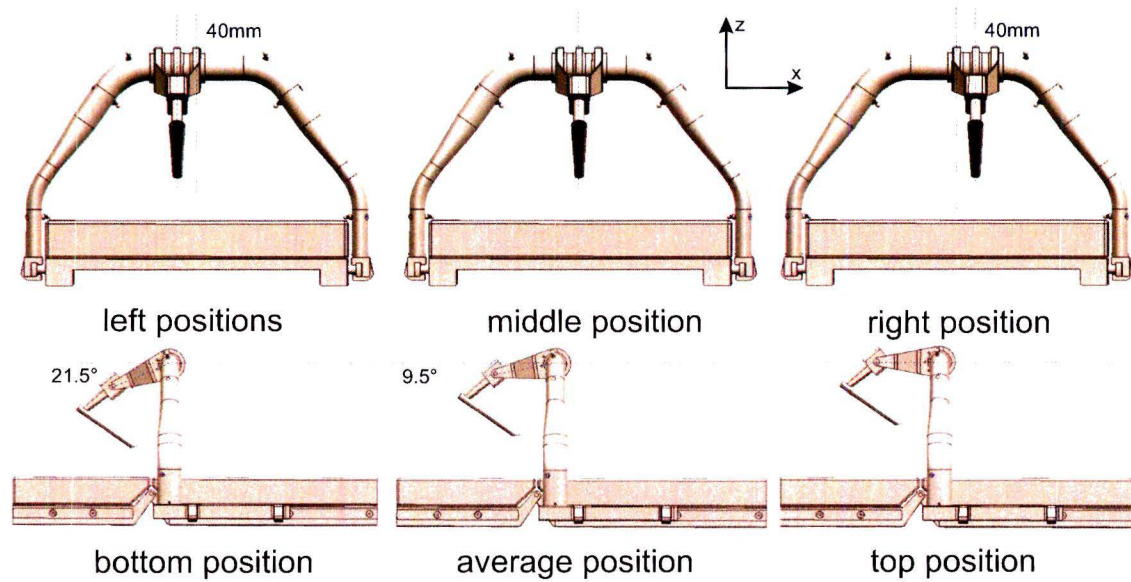
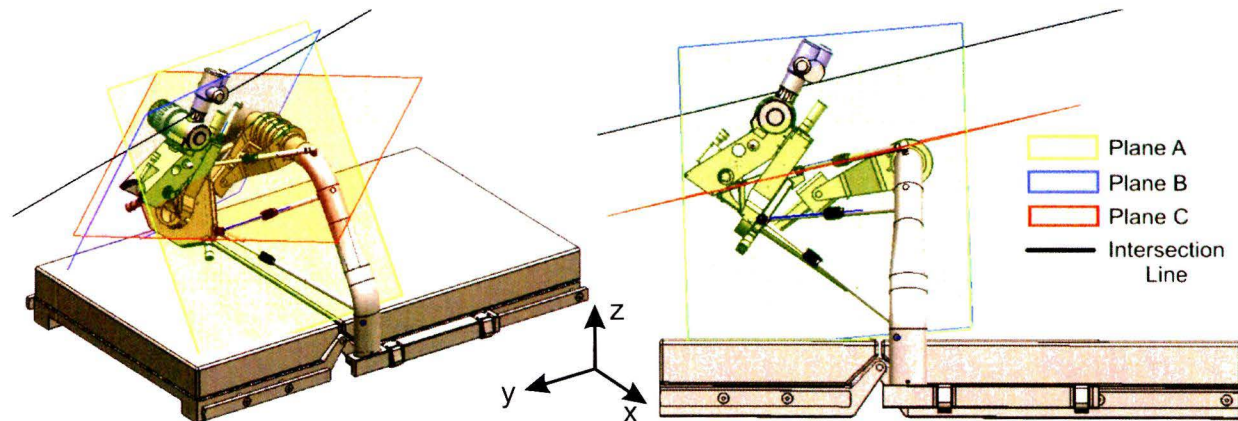


Figure 3.8: Laryngoscope arm in its maximum positions for  $x$  and  $\phi$

### 3.5 Support Rods

The support rods are used to support the weight and hold the laser tool in place. The support rods are used as A-frames so from two points on the frame two support rods go to one point on the laser tool. Each rod will fix one DOF therefore to fix the six DOF of the laser tool six rods are needed which will act as three A-frames. There is one extra condition for the three A-frames, when all the rods will point to one point a pole is created around which the body can rotate. Therefore the following design rule has to be taken into account. The planes of the first two a frames have an intersection line now the third plane has to be parallel to this intersection line, if not the intersection of the line and the plane will create the pole around which the body still can rotate.

In figure 3.9 the frame with the support rods is drawn. Also the planes and the intersection line are shown. In this figure it becomes clear that planes A and B span the intersection line and that plane C is parallel to this intersection line. Therefore the laser tool is fixed.



**Figure 3.9:** Frame assembly with three A-frame planes (red, green, blue) and intersection line (black)

The connection rods are fixed to the frame with ball joints. The other ends of the rods are fixed to the laser tool with ball joints. Only this time two rods are fixed to one ball such that the centerlines of the rods cross each other and this crossing lays on the centerline of the ball joint. The support rods are also made adjustable in length. This is done because every patient is different (one is bigger than the other) and it is impossible to lay the patient every time exactly in the middle of the table. In theory the A-frame should be able to reach every point in space, but in practice this is limited by the length of the rods and the range of the ball hinges. The range of the rods will not limit surgery because for the average patient described in section 2.3 the hinges and the length of the rods are in the middle of their range therefore they have maximum adjustments to both sides of the range.

The length adjustment of the support rods is achieved by letting a rod slide in a bigger tube. In order to fix the laser tool in place this sliding motion should be lockable. In figure 3.10 the locking mechanism is shown. The locking function is achieved with a collet chuck. The collet is machined on the outer tube and the chuck is made like a bnc connector such that the support rod can be locked with only a quarter of a turn of the chuck. On the tube with the collet two pins are placed and in the chuck a profile is cut such that the chuck is pulled down by the pins when it is rotated.

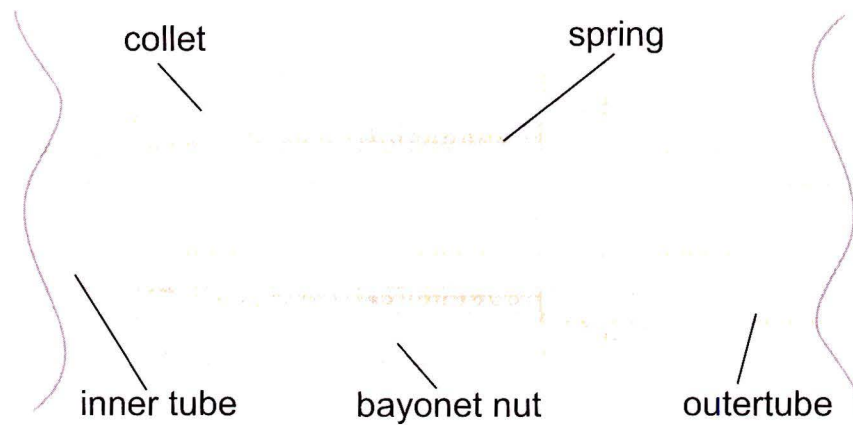


**Figure 3.10:** *Cross-section of the bayonet closing*

To put the lasertool in place during surgery the next procedure has to be followed. First all the connection rods have to be unlocked. Then they have to be connected with one end to the frame and the other end to the lasertool. Now the lasertool can be put in place on top of the opening of the laryngoscope. When the lasertool is in place the connection rods can be locked on the laser tool is fixed.



## Chapter 4

# Laser Tool

### 4.1 Introduction

In this chapter the design and the functionalities of the laser tool are discussed. In the first part the manipulation of the laser tool will be discussed elaborately. In this case the term manipulation is used for the positioning of the laser tool tip onto the tumor. In figure 4.1 the directions of the DOF's with respect to the laryngoscope are presented. The manipulator of the laser tool is divided into two modules. The first module contains the manipulation for the  $x, y, \theta$  and is discussed in section 4.2. The second module is the  $z$ -manipulator which is stacked on the  $x, y, \theta$ -manipulator, the  $z$ -manipulator is discussed in section 4.3. On top of the  $z$  manipulator the AcuBlade™ with the tool attached is mounted. The combination of the AcuBlade™ with the tool will be referred to as the cutting tool and is explained in 4.4.

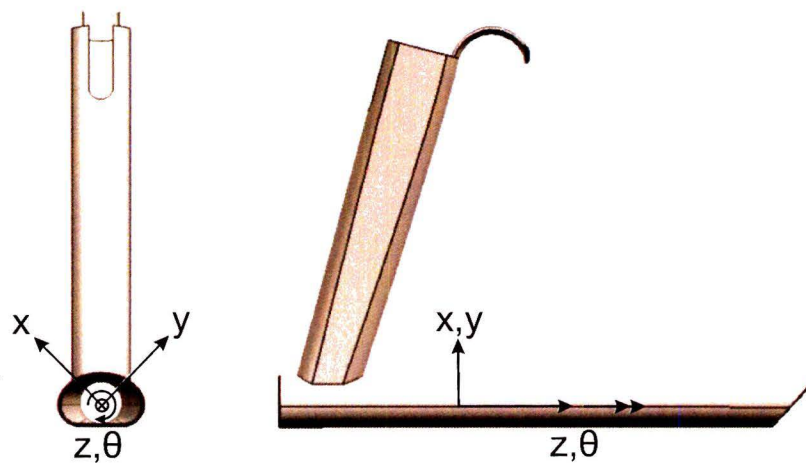


Figure 4.1: Definition of the coordinate system with respect to the laryngoscope



## 4.2 $x, y, \theta$ -Manipulator

### 4.2.1 Concept

The adjusting possibilities of the cutting tool should be stacked as little as possible. Stacking different manipulators can result in hysteresis. For example a platform is fixed on top a manipulator for the  $y$ -direction and this  $y$ -manipulator is fixed on a manipulator for the  $x$ - direction which is fixed to the world (figure 4.2a). Assuming both manipulators are identical and have a little play perpendicular to the manipulating direction and there is no play in the manipulation direction. Now the play will result in hysteresis in both the  $x$  and  $y$  direction. An other way of manipulating is shown in 4.2b. Both manipulators are fixed to the world and the platform is fixed to the manipulators. The platform is fixed to the manipulator such that it is free in the direction perpendicular to the manipulation direction. When there is play in one of the manipulators it will not affect the position of the platform that is adjusted with the other manipulator.

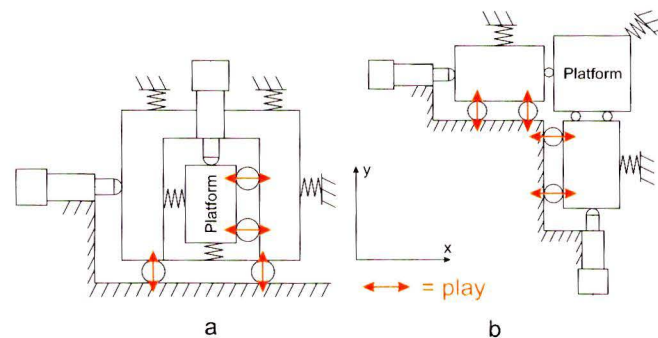


**Figure 4.2:** Schematic representation of an  $x, y$ -manipulator stacked (serial) (a) and parallel (b)

From 4.2b the following concept for the  $x, y, \theta$ -manipulator was designed. The concept is shown in figure 4.3. A proximal plate should be placed in front of the laryngoscope with a hole in it which has the shape of the laryngoscopes opening. On this plate the mechanism of figure 4.2b is built but now the square platform is replaced with a round flange. Now the  $x, y$  can be manipulated and because of the round flange the  $\theta$  is also still free such that it can be manipulated.

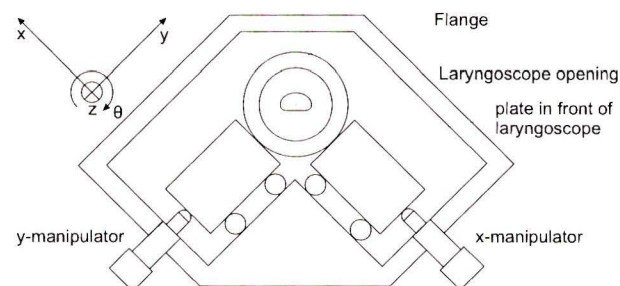


**Figure 4.3:** Schematic representation of the concept for the  $x, y, \theta$ -manipulator

This concept is further developed in the next section where the final for the  $x, y, \theta$ -manipulator design is shown.

#### 4.2.2 $x,y,\theta$ -Mechanism

Figure 4.4 shows the final  $x,y,\theta$ -manipulator. In this figure the flange which is manipulated and on which the z-manipulator is placed can be seen. Also the ball joints which are used to mount the manipulator to the frame and the microscrews (Standa 9S75M-10\_AL [9]) to make adjustments in the x- and y-direction can be seen in this figure. The  $\theta$  is used to position the suction tube such that it is not in the way, this is necessary because of the design of the cutting tool. The cutting tool is only able to cut an arc of  $200^\circ$ . To cut a full circle the whole tool should be rotated  $180^\circ$  after the first  $200^\circ$  are cut to cut the rest of the circle. On the back of the  $x,y,\theta$  manipulator there are five locating pins. These locating pins are used to locate the  $x,y,\theta$ -manipulator on the laryngoscope such that the opening of the manipulator is exactly in front of the laryngoscope opening.

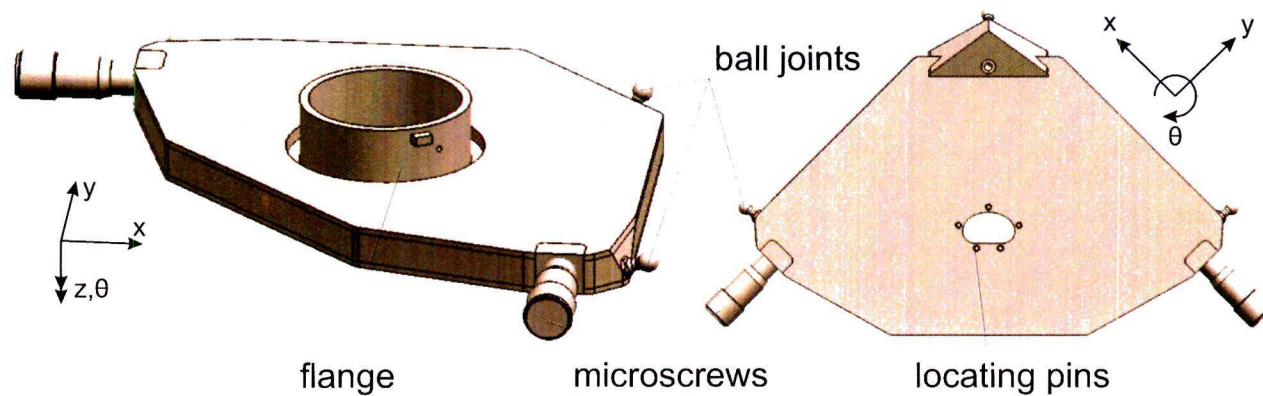


Figure 4.4: 3D (left) and back view (right) of the  $x,y,\theta$ -manipulator

To further discuss the  $x,y,\theta$ -manipulator figure 4.5 shows the manipulator without the top plate such that the mechanism is exposed. In this figure it becomes clear that the slides shown in the concept of figure 4.3 are replaced by parallelograms. This is done to make it more compact and a parallelogram has less friction. The parallelogram is built up with two swingarms per pivot point one on the top side of the adjustment arm and one on the bottom. Now a sandwich construction is created. The pivot point on the other end of the swing arm is fixed to the housing wall. The flange is resting on a thickened part of the bottom plate and on both adjustment arms. The thickened part is to lift the flange to the same height as the adjustment arms. The flange is pretensioned against both adjustment arms with a bending spring. This spring is fitted over a springpin that is fixed to the bottom and top plate. The force of the spring is acting along the line of the two contact points. These forces are shown in red in figure 4.5.

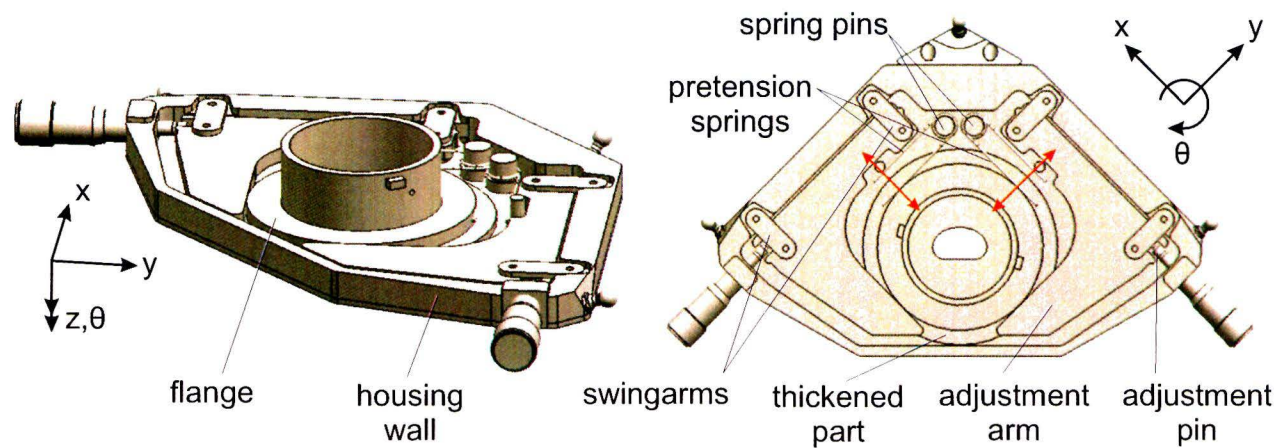


Figure 4.5: 3D (left) and top view (right) of the  $x,y,\theta$ -manipulator without the top plate

The micro screws for  $x$  and  $y$  adjustments are pushing against the adjustment pins that are screwed in the adjustment arm. When a line is drawn perpendicular to the centerline of the adjustment pin, from the point where it is screwed into the adjustment arm the line will cross the midpoint of the flange. This is shown in figure 4.6. This property makes it virtually pushing against the midpoint of the flange. The hole in which the adjustment pin is fitted is large enough to allow the adjustment pin to bend elastically. This to allow the parasitic movement that is induced by the parallelogram mechanism perpendicular to the adjustment direction. This parasitic movement has a maximum of  $1.09\text{mm}$ .

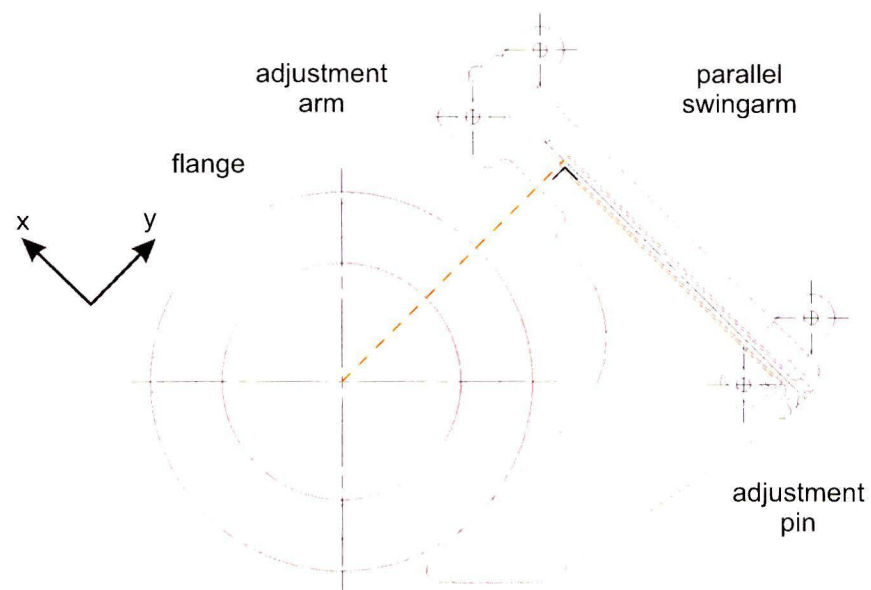
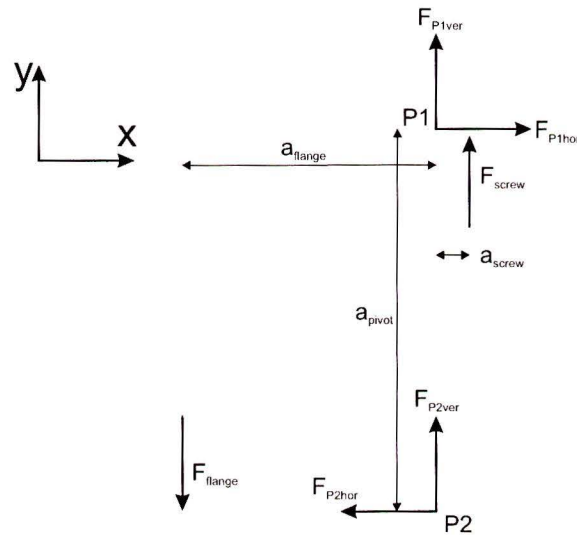


Figure 4.6: Cross-section of the adjustment arm with swing arms and adjustment pins connected

The places where the forces are acting on the adjustment arm are chosen carefully. They are chosen such that the mechanism is never going through the play in the pivots of the parallelogram. This is shown in figure 4.7 from this figure the force equilibrium is determined and shown in equations 4.1 and 4.2.



**Figure 4.7:** Freebody diagram of an adjustment arm

The moment equilibrium with P1 as pivot point

$$a_{flange} F_{flange} + a_{screw} F_{screw} = a_{pivot} F_{P2hor} \quad (4.1)$$

The moment equilibrium with P2 as pivot point

$$a_{flange} F_{flange} + a_{screw} F_{screw} = a_{pivot} F_{P1hor} \quad (4.2)$$

$F_{flange}$  and  $F_{screw}$  will never change direction because neither is able to pull on a contact they can only push (they can be zero). This makes the left term in equations 4.1 and 4.2 always positive which automatically means that the right term will never change sign. So the force in the swingarms is never changing direction so the mechanism will never go through the play in the pivot points. From this also can be concluded that the swingarm connected to pivot 1 will be under tension and the swing arm connected to pivot 2 under compression force.

## 4.3 z-Manipulator

### 4.3.1 Concept

For the z-manipulator it is important that it moves along a straight line. This is important because when the laser tool is pointed at the tumor the tool has to be lowered towards it. When this is not done along a straight line the tool will not end at the point to which it was aimed at.

The range needed for the z-manipulator can be determined by the thickness of the tool especially the suction tube and the line of sight past it. A schematic representation of this is shown in figure 4.8. Here only the last piece of the suction tube is shown with the dotted line as the line of sight.

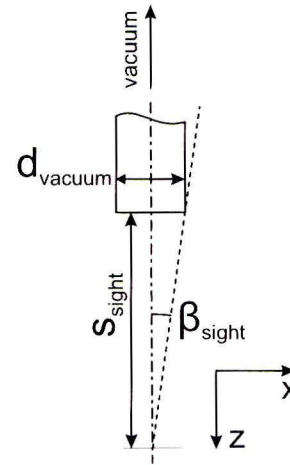


**Figure 4.8:** Schematic representation of the line of sight past the suction tube

In this figure  $d_{vacuum} = 1mm$  is the diameter of the suction tube and  $\beta_{sight} = 4.46^\circ$  is the minimal angle of sight which is possible through the tube. From this information follows  $s_{sight} = 6.4mm$ . The range needed for z should be at least  $6.4mm$ . To compensate for deviations from this schematic situation a z-range of  $10mm$  is chosen.

Figure 4.9 shows the first concept for a z-manipulator. The crank is fixed to the world in point A with freedom in  $\psi$  and it is fixed to the swingarm in point C also with freedom in  $\psi$ . The swingarm is fixed to the world in point B with freedom in  $\psi$ , point B is fixed in a slide which has freedom in x. The lines AC, BC and CD are of equal length R. When the slide of point B is moved in the x-direction point D will move along a straight line in the z-direction.

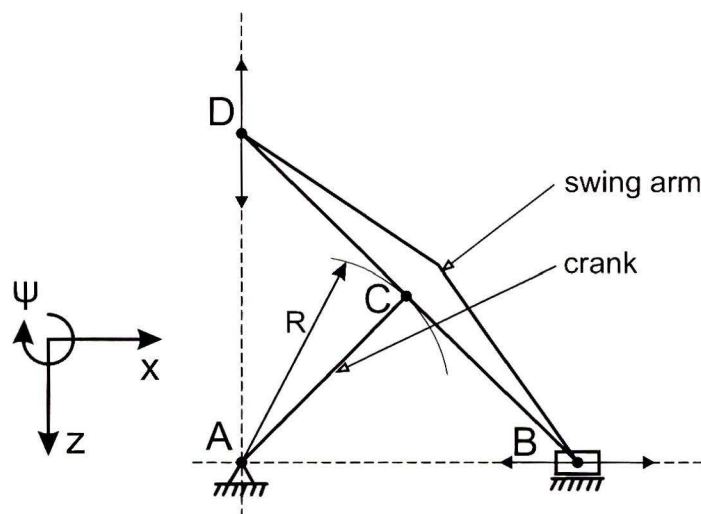


**Figure 4.9:** Concept for guiding a point along a straight line inspired by a ladder against the wall [8]



### 4.3.2 Mechanism

In figure 4.11 the final mechanism used as z manipulator is shown. Figure 4.12 shows the same mechanism but now with some parts made translucent. In this figure the points of rotation are similar as the concepts described in the previous section only some points of rotation are doubled for stiffness in other the directions. The double points of rotation have the same letter but are numbered with a subscript. In this figure it becomes clear that the rotation points A, C, D, F and G are doubled. Points A, D and G are placed as far apart as needed to keep the opening of the laryngoscope and of the  $x,y,\theta$ -manipulator clear.

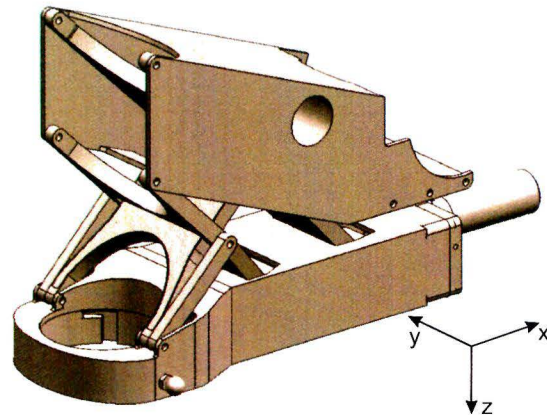


Figure 4.11: Overview of the final mechanism for the z-manipulator

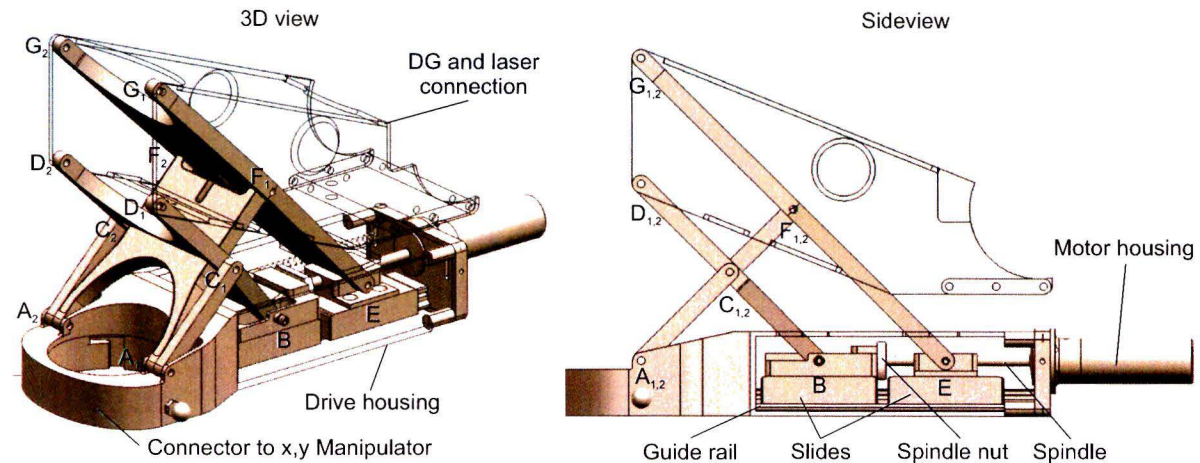


Figure 4.12: 3D and sideview of the z manipulator mechanism with parts made translucent

The stiffness of the laser connection in the z-direction is the axial stiffness of the spindle drive (the spindle drive is discussed in section 4.3.3). The other slide is not contributing to the stiffness in this direction because it is free in the axial direction (x) of the spindle. The stiffness perpendicular to the rail of the slide at point E is giving the laser connection stiffness in  $\theta$ . This point is giving stiffness because it has the largest distance from the mounting point D and G on the laser connection that has to be kept in place. For x and  $\psi$  the bending stiffness of the swingarm with the lowest stiffness is determining. Since the length of the component is in the stiffness with the power -3 the longest swingarm is probably the one with the lowest stiffness and therefore the determining component in these directions. So swingarm

EG is supplying stiffness in  $x$  and  $\psi$ . The distance between  $A_1$  and  $A_2$  is determining for the stiffness in the  $y$  and  $\phi$  direction. This is because these are the only points which have distance in the  $y$  direction and are fixing the mechanism to the world.

The laser connection is a tube with a rectangular cross-section with holse milled into the walls to put the singarms and cranks through. This tube is used to mount the laser cutting tool to the point D and G. To increase the torsional stiffness of this rectangular tube a circular tube is welded in it as can be seen in figure 4.11.

The rail and slide shown in figure 4.12 come from SKF and the type number is LLMWS 12 TA [10]. The slides to point B and E can move separately. Two slides are needed because due to the difference in size between the two separate mechanisms they will not make the same motion. In this case a motion is put on slide B and slide E can move freely on the rail. The spindle drive is discussed elaborately in in the next section.

The swingarms BD and EG and crank AF are made hollow this is shown in figure 4.13. This figure shows the swing arm with and without cover as an example. This cover is put on the open side of the swingarm to create a closed box structure for extra stiffness. When hollowing out some walls have to stay up. When these walls are chosen such that they are in the same direction as the forces acting in the arm, the arm will not lose to much stiffness. The advantage of hollowing out the arms is weight reduction and when the walls are chosen well the weight/stiffness ratio will improve.

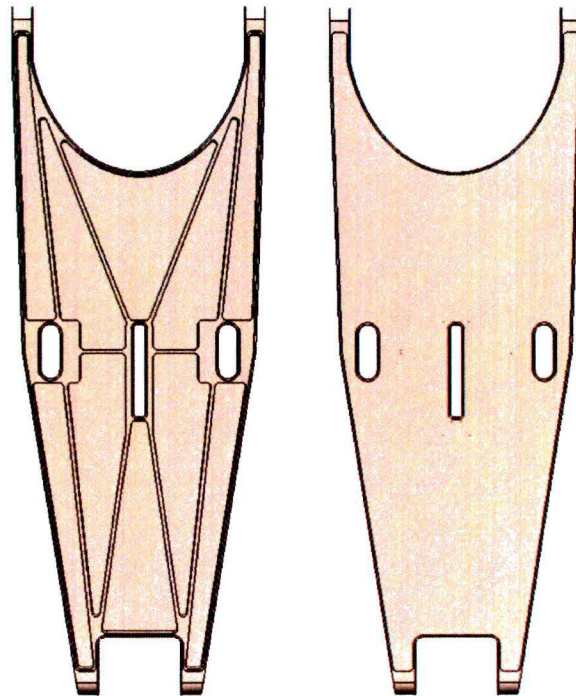


**Figure 4.13:** Walls that are left to keep stiffness but reduce weight in swingarm EG (left) with cover (right)

The  $x,y,\theta$ -connector is used to connect the  $z$ -manipulator to the flange sticking out of the  $x,y,\theta$ -manipulator. This is a bayonet closure which has a locking pin such that the bayonet also locks the  $\theta$  of the  $z$ -manipulator with respect to the flange. This lock is needed because this rotation is the  $\theta$  of the  $x,y,\theta$ -manipulator. Therefore to prevent  $z$ -manipulator from coming loose the locking pin is needed. The size of the hole in the connector to the  $x,y,\theta$ -manipulator is conform the criteria described in section 4.1.



### 4.3.3 Actuation

The actuation will be done on point B (figure 4.12). The swing arm BD and crank AC are the shortest and therefore the most stiff crank and swingarm. Appendix A.1 shows the relation between the x displacement of point B and the z displacement of point D and therefore also point G. In this figure it can be seen that this relation is not linear this can be compensated with the motion of point B.

To design an actuation for the z manipulator the force needed for lifting and lowering has to be calculated. Figure 4.14 shows the free body diagram of the laser mounting tube. Where  $F_z$  represents the gravity force of the AcuBlade™ module and  $F_{GH}$ ,  $F_{DH}$ ,  $F_{DV}$  the forces at the connection points D and G. Equations 4.3, 4.4 and 4.5 give the force equilibrium of this free body diagram.

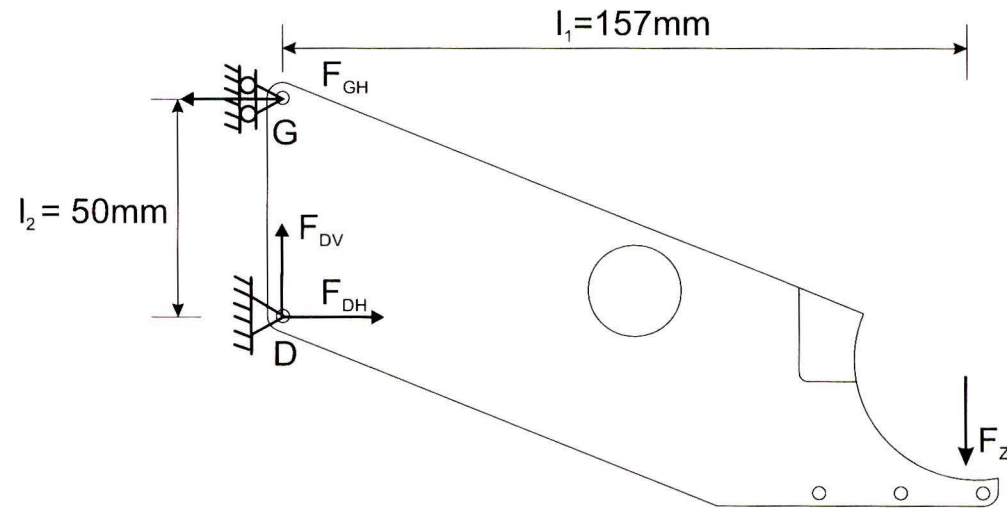


Figure 4.14: Free body diagram of laser mounting tube

$$\sum F_H = -F_{GH} + F_{DH} = 0 \quad (4.3)$$

$$\sum F_V = -F_z + F_{DV} = 0 \quad (4.4)$$

$$\sum M_D = l_1 F_z - l_2 F_{GH} = 0 \quad (4.5)$$

The solution to this force equilibrium is given by equations 4.6, 4.7 and 4.8.

$$F_{GH} = \frac{l_1}{l_2} F_z \quad (4.6)$$

$$F_{DH} = \frac{l_1}{l_2} F_z \quad (4.7)$$

$$F_{DV} = F_z \quad (4.8)$$

Now the forces on the swingarm can be calculated. Therefore the free body diagram of the swingarm BD is presented in figure 4.15. In this figure  $F_{act}$  is the needed actuator force and  $F_{BV}$  and  $F_C$  are the other forces on the nodes. In equations 4.9, 4.10 and 4.11 the force equilibrium of this free body diagram is presented. In equation 4.12  $\beta$  as function of  $x$  is presented.

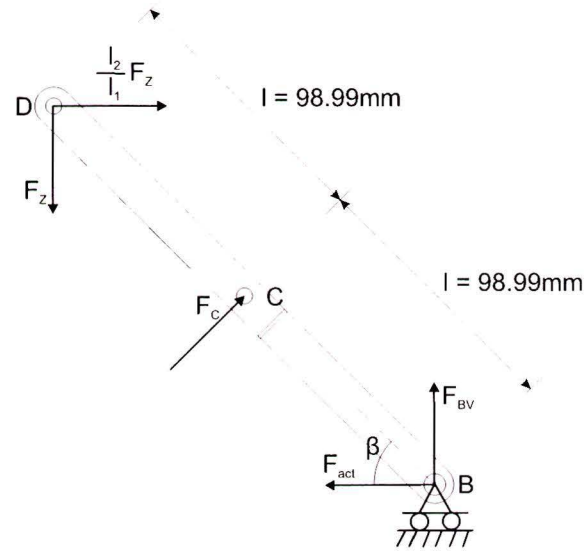


Figure 4.15: Free body diagram of swingarm BD

$$\sum F_H = F_{act} + \frac{l_1}{l_2} F_z + F_c \cos \beta = 0 \quad (4.9)$$

$$\sum F_V = F_{BV} - F_z + F_c \sin \beta = 0 \quad (4.10)$$

$$\sum M_D = -l F_c - 2l F_{BV} \cos \beta + 2l F_{act} \sin \beta = 0 \quad (4.11)$$

$$\beta = \cos^{-1} \left( \frac{2l}{l_0 + x} \right) \quad (4.12)$$

The result of these equation is shown in appendix A.2.

The maximum actuation force needed is 8.1N. This force can easily be achieved with an spindle and motor. The spindle chosen has a diameter of 4mm a lead of 1mm and can take an axial load of 50N (datasheet [11]). With the data of the chosen spindle the needed actuation torque can be calculated with equations 4.13, 4.14, 4.15 and 4.16 [12]. Where in equation 4.13  $l$  is de lead in [mm]  $d_m$  the mean diameter of the screw in [mm] and  $\alpha$  is the helix angle. In equation 4.14  $\mu_{spindle}$  is the friction coefficient and  $\phi_{spindle}$  is the friction angle in [°]. Equations 4.15 and 4.16 represent the torque needed to lift of lower the slide. Where  $W$  is the axial force needed ( $F_{act}$ ).

$$\alpha = \tan^{-1} \left( \frac{l}{\pi d_m} \right) \quad (4.13)$$

$$\mu_{spindle} = \tan \phi_{spindle} \quad (4.14)$$

$$M_{lifting} = \frac{W d_m}{2} \tan(\phi + \alpha) \quad (4.15)$$

$$M_{lowering} = \frac{W d_m}{2} \tan(\phi - \alpha) \quad (4.16)$$

In appendix A.3 the torque needed to lift or lower the load on the spindle. The following parameters are used.  $l = 1mm$ ,  $d_m = 3.65mm$ ,  $\mu_{spindle} = 1$  and  $W = F_{act}$ .

From this can be concluded that the maximal motor torque needed is  $0.0179Nm$ . This torque can be accomplished with a maxon RE 13 with model number 118416 motor [13] and maxon GP 13 A with model number 352367 planetary gear head [13]. The maximal torque that the motor can generate is  $0.5mNm$ . Together with the gearbox which has a transmission ratio of 131:1 and an efficiency of 0.75 this results in an output torque of  $0.049Nm$ . The maximal torque of the gearbox is  $0.3Nm$ . So the motor/gearbox combination can generate plenty of torque to lift and lower the load while staying within the motor and gearbox limits. The high reduction ratio does not only result in a high output torque with a small motor but also the motor can run at a higher speed. When the motor runs at a high speed it has a more constant torque. For the z a speed of  $1mm/s$  is wanted this is achieved with a rotational speed of the motor of  $7860rpm$ .

Figure 4.16 shows the final design of the actuation of the z-manipulator. This figure shows that the nut is fixed to the slide which contains point B such that the centerline of the spindle crosses through pivot point B. The spindle is fixed to a flange on one end and is free at the other end. This is such that the spindle is following the slide better. This flange is guided with an axial bearing which is between the flange and the end block, the bearings of the gearbox are used as radial bearings. The spindle and axial bearing are pretensioned with two springs placed between the end block and slide B. Around the motor and the gearbox a cover is placed such that the motor and electrical wires cannot be contaminated.

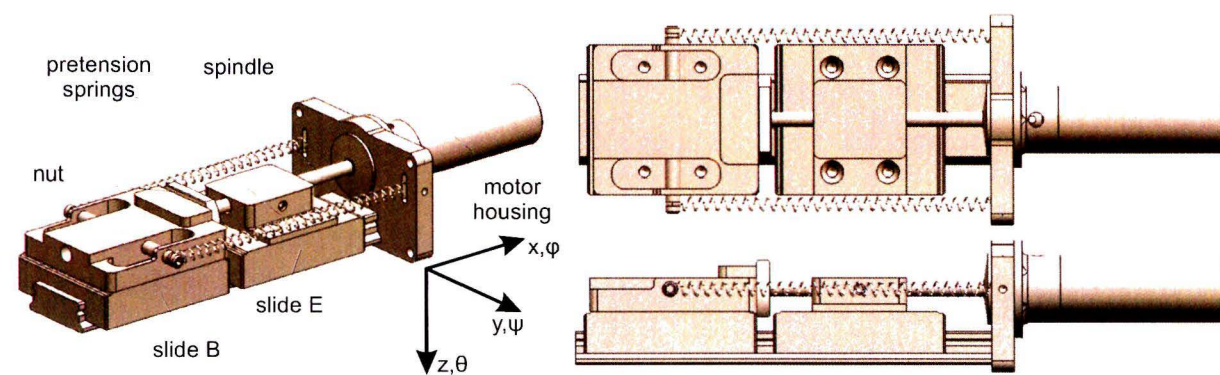


Figure 4.16: Drive unit of the z-manipulator

## 4.4 Cutting Tool

### 4.4.1 Concept

Figure 4.17 shows the concept for the cutting tool. The tumor is grabbed with a suction tube which is connected to a vacuum pump. Next to the suction tube is a mirror which angle ( $\psi$ ) can be adjusted and the mirror can rotate around the suction tube ( $\theta$ ). With the rotation around the suction tube a cut around the tumor can be made, the angle adjustment ( $\psi$ ) of the mirror makes it possible to gradually cut under the tumor. The possibility of cutting under the tumor makes that less healthy tissue is cut away during surgery. This is also shown in figure 4.17, (a) is the starting situation and gradually the laser will cut under the tumor to situation (e) where the tumor is removed. The advantage of leaving more healthy tissue is that the risk of loss or change of voice is less.

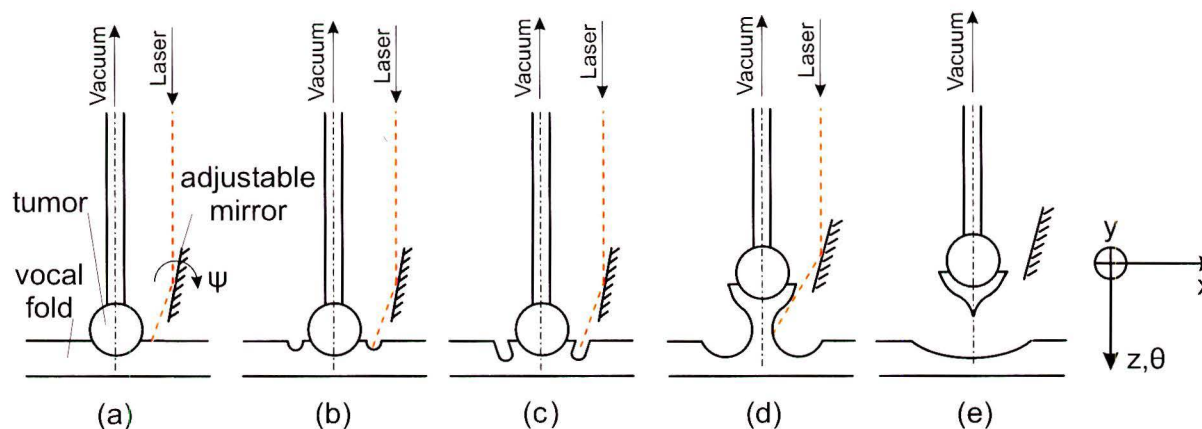
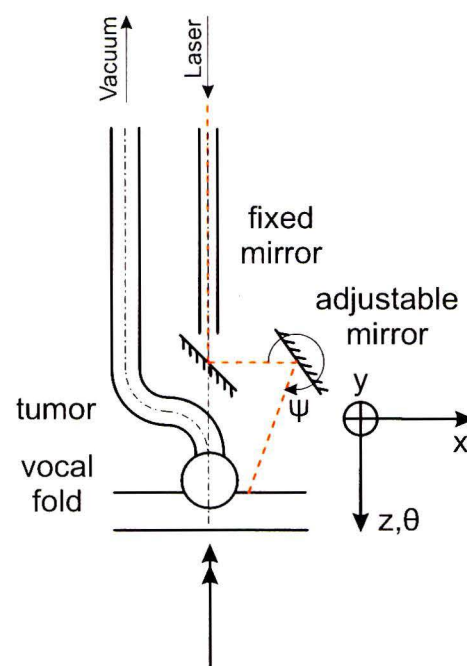


Figure 4.17: Concept for the design of the cutting tool which is cutting gradually under the tumor (a) to (e)

In the concept shown in 4.17 the laser rotates around the suction tube. The problem with that is that the laser is going down the laryngoscope along the suction tube unprotected. When a cover is put over the laser (for example a tube) this tube has to follow the direction of the laser. So the tube has to make the same movements as the laser beam. While the suction tube stays in place. Therefore it is much easier to use the tube of the laser as the shaft to rotate around and put the tube with the vacuum off the centerline. This new concept is shown in figure 4.18. In this figure both mirrors are fixed to that tube protecting the laser. The fixed mirror is completely fixed to the tube and the adjustable mirror still has one DOF free to adjust the angle  $\psi$  of the mirror and thus the distance of the cut with respect to the tumor. This concept is elaborated upon in the following section.



**Figure 4.18:** Concept with the laser over the axis of rotation and the tube with the vacuum parallel

#### 4.4.2 Cutting Tool Tip Mechanism

Figure 4.19 shows the final mechanism chosen for the cutting tool tip. The tube for the laser is used to fix the cutting tool tip to the frame and to cover the laser beam. Next to the laser tube is the suction tube to which the vacuum pump should be connected. In this design one mirror is fixed to the tube and the other is fixed on an arm (mirror arm) for actuation, this arm is free in the  $\psi$ . The mirror arm has a pivot point with a shaft that lays in two v-blocks. The mirror arm is actuated via a wedge which can move in  $z$ . The actuation of the wedge is done via a pushpull rod which also runs parallel to the tube for the laser. When the wedge moves the mirror arm will follow the slope of the wedge and thus the angle of the adjustable mirror is adjusted.

The tool tip has three DOF's the first is  $\theta$  around the tube for the laser. This DOF is used to rotate the adjustable mirror around the tube for the laser such that an arc around the tumor can be cut. The second DOF is  $\theta$  around the suction tube this is used to rotate the tool tip away from the tip of the suction tube. Such that the tip of the tube can be aimed at the tumor before it is lowered towards it with the  $z$ -manipulator. The last DOF is  $\psi$  of the mirror arm. This is used to adjust the mirror angle and thus the distance of the laser beam bundle from the tumor.

The mirrors used have to be made of gold. Or at least the surface of the mirrors have to be made of gold. This is due to the used laser. The AcuPulse™ is a CO<sub>2</sub> type of laser. The light emitted by the laser has a wave length of  $10.6\mu m$  which is in the infrared spectrum. Infrared light requires special materials for optics. In this case the material gold is chosen because it has a high reflectivity and it has been used more often in medical appliances.

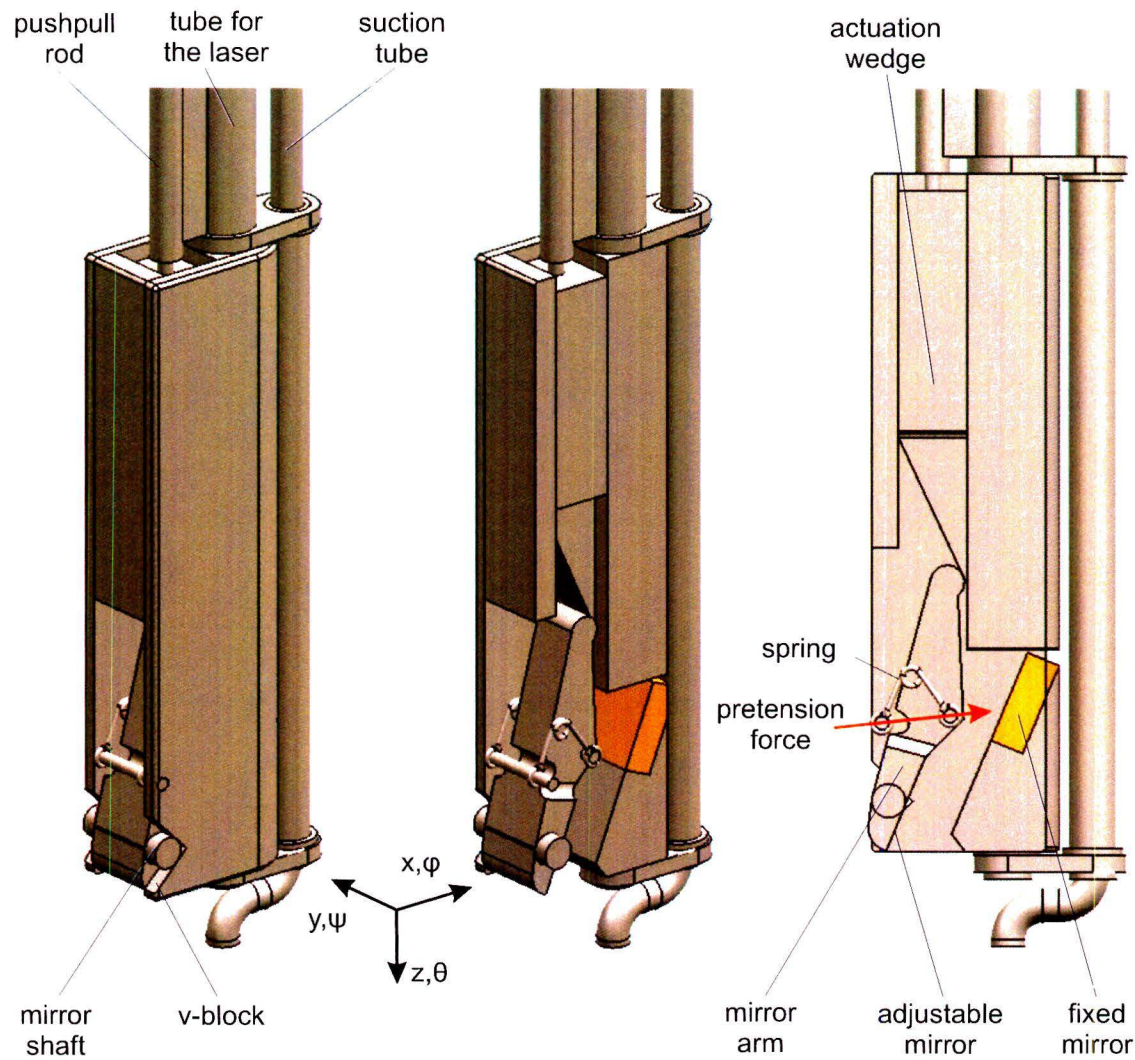
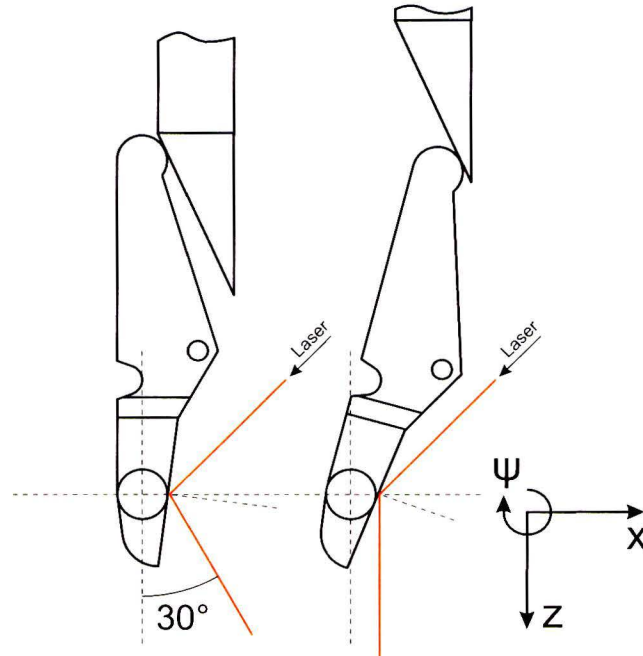


Figure 4.19: Final mechanism of the cutting tool tip

The size of the mirrors has to be determined such that the laser will never go of the mirror, which may result in unwanted cuts or reflections. For the fixed mirror only the surface of the laser beam on the mirror has to be calculated. When this dimension is correct the laser will never miss it because this mirror stays in place. Hence for the mirror on the mirror arm it becomes slightly more complicated. Because it has an adjustable angle. Therefore the size of the surface of the laser beam on the mirror will vary and the mirror surface is not on the centerline of the shaft which will result in the laser beam walking over the mirror when the angle  $\psi$  is adjusted. Assumed is that cutting will be done with a laser beam with a cross section of  $t_{laser} = 0.4mm$  and  $w_{laser} = 1mm$

Figure 4.20 shows the mirror arm in its minimum and maximum position. This figure shows that due to the fact that the mirror surface is not crossing the centerline of the mirror arm shaft, the laser beam is moving over the mirror. The dimensions of the mirror depends on the size of the laser beam on the mirror, thus of the angle of the mirror with respect to the laser beam and the maximum walk of the laser beam over the mirror. Therefore the minimum mirror height is given by equation 4.17. Where  $h_{laser_{max}}$  is the maximum laser height on the mirror and  $x_{walk_{max}}$  is the maximum distance the laser beam will walk over the mirror.



**Figure 4.20:** Mirror arm in its minimum (left) and maximum (right) position

$$h_{mirror_{min}} = h_{laser_{max}} + x_{walk_{max}} \quad (4.17)$$

Figure 4.21 zooms in on the mirror surfaces of figure 4.20. In this figure the minimal angle of the mirror is named  $\zeta_0$ ,  $x_0$  is the distance from the centerline of the laser beam to the horizontal line through the center of the mirror arm shaft.  $r_0$  is the radius of the mirror arm shaft.  $\zeta_n$  and  $x_n$  give the mirror angle and distance from the horizontal line for any arbitrary point in the range for  $\zeta$ . Equations 4.18, 4.19 and 4.20 gives the relation between the mirror angle ( $\psi$ ) and the maximum distance  $x_{walk}$  the laser will walk over the mirror.

$$x_0 = r_{shaft} \tan(\zeta_0) \quad (4.18)$$

$$x_n = r_{shaft} \tan(\zeta_n) \quad (4.19)$$

$$x_{walk} = x_n - x_0 = r_{shaft} (\tan(\zeta_n) - \tan(\zeta_0)) \quad (4.20)$$

In this design  $r_{shaft} = 1mm$ ,  $\zeta_0 = 7.5^\circ$  and  $\zeta_{max} = 22.5^\circ$  which results in a  $x_{walk}$  as shown in appendix B.1. This figure shows  $x_{walk}$  as function of  $\zeta$ . The maximum value for  $x_{walk}$  is  $0.28mm$  this is determining for the minimal mirror dimension.

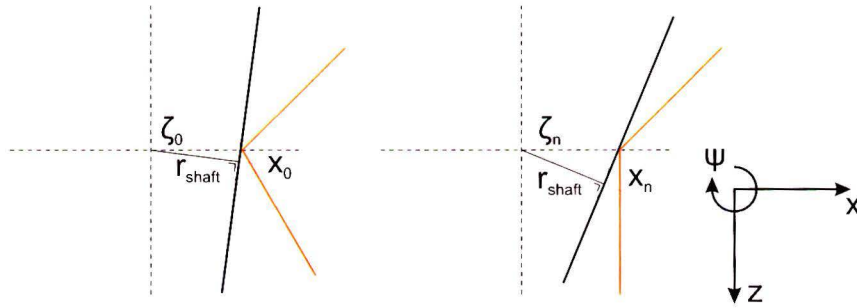


**Figure 4.21:** Zoomed in on the mirror surface of figure 4.20, left minimum position and right maximum position

In figure 4.22 a schematic representation of the mirror and the shaft to calculate the laser height on the mirror as function of  $\zeta$  is shown. Equation 4.21 shows the relation between laser height  $h_{laser}$  and angle  $\zeta$ .

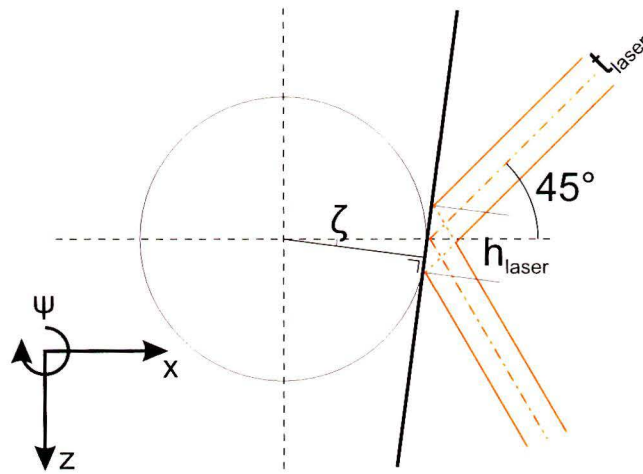


**Figure 4.22:** Schematic representation of the height of the laser beam

$$h_{laser} = \frac{t_{laser}}{\sin(45^\circ - \zeta)} \quad (4.21)$$

The result of equation 4.21 is shown in appendix B.2 where  $h_{laser}$  is given from  $\zeta_0 = 7.5^\circ$  to  $\zeta_{max} = 22.5^\circ$  is shown. The maximum value for  $h_{laser}$  is  $1.05mm$  which is also determining for the minimal size of the mirror

Now the minimum mirror height is calculated with equation 4.17 the result is  $h_{mirror_{min}} = 1.33mm$ . The fixed mirror is under an angle of  $22.5^\circ$  with respect to the laser beam. This results in a  $h_{laser}$  on the fixed mirror of  $1.05mm$ . The laser has a width (in  $y$ ) of  $1mm$  on both mirrors. With this information the following dimensions for the mirrors are chosen. The fixed mirror has a surface of  $2 \times 2mm$  and the adjustable mirror has a width of  $2mm$  and a height of  $3mm$ .



Now the mirror arm has to be pretensioned against the adjustment wedge. The direction and magnitude of the force have to be correct. The direction of the force is given in figure 4.19. This direction is constructed with Wittgens graphical methode [8]. In appendix B.3 and B.4 Wittgens methode is shown for the minimal ( $\zeta = 7.5^\circ$ ) and the maximal ( $\zeta = 22.5^\circ$ ) mirror angle. With Wittgens method also the orientation of the v-block is chosen as it is.

The force is calculated with the following procedure. The springs have to keep the the mirror arm in place when it is exerted at its eigenfrequency. The eigenfrequency can be estimated as follows, assuming there is no damping in the cutting tool shaft the eigenfrequency  $f_n$  is given by equation 4.22. Where  $k$  is the bending stiffness of the cutting tool shaft and  $m$  the mass of the cutting tool.

$$f_n = \frac{1}{2\pi} \sqrt{\frac{k}{m}} \quad (4.22)$$

The mass is estimated assuming that the tool tip is one solid piece of metal. This is assumed because this is the maximum weight possible in this volume which is the worst case scenario. The tool tip has a volume of  $3.4 \times 5.5 \times 20 = 374 \text{ mm}^3$ , when the material is stainless steel  $\rho = 8000 \text{ kg/m}^3$  the mass becomes  $m = 3 \text{ g}$ . Bending stiffness  $k$  is given by equation 4.23 where  $I$  is the second moment of area of the cutting tool shaft,  $L$  is the length of the cutting tool shaft and  $E$  is the elasticity modulus of stainless steel.

$$k = \frac{3EI}{L^3} \quad (4.23)$$

To estimate  $I$  figure 4.23 shows a schematic representation of the cross section of the cutting tool shaft. Equations 4.24, 4.25, 4.26, 4.27 and 4.28 give the calculation of  $I$ . With the following parameters  $I = 8.16 \cdot 10^{-12} \text{ mm}^4$  is calculated.  $D_{pushpull} = 1 \text{ mm}$ ,  $a_{pushpull} = 2.35 \text{ mm}$ ,  $b_{con} = 1 \text{ mm}$ ,  $h_{con} = 0.7 \text{ mm}$ ,  $a_{con} = 1.5 \text{ mm}$ ,  $D_{laserin} = 1.5 \text{ mm}$ ,  $D_{laserout} = 2 \text{ mm}$ ,  $D_{laser} = 0.15 \text{ mm}$ ,  $D_{vacin} = 0.8 \text{ mm}$ ,  $D_{vacout} = 1 \text{ mm}$  and  $a_{vac} = 2.35 \text{ mm}$

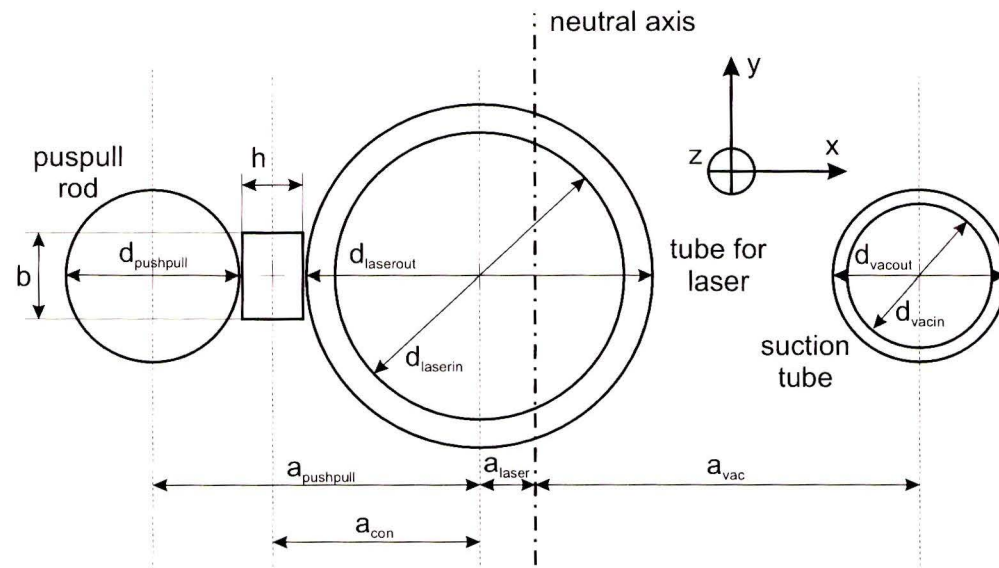


Figure 4.23: Schematic cross-section of the laser cutting tool shaft

$$I = I_1 + I_2 + I_3 + I_4 \quad (4.24)$$

$$I_1 = \frac{\pi D_{pushpull}^4}{64} + \frac{\pi D_{pushpull}^2}{4} a_{pushpull} \quad (4.25)$$

$$I_2 = \frac{b_{con} H_{con}^3}{12} + b_{con} H_{con} a_{con}^2 \quad (4.26)$$

$$I_3 = \frac{\pi (D_{laserout}^4 - D_{laserin}^4)}{64} \quad (4.27)$$

$$I_4 = \frac{\pi (D_{vacout}^4 - D_{vacin}^4)}{64} \frac{\pi (D_{vacout}^2 - D_{vacin}^2)}{4} a_{vac}^2 \quad (4.28)$$

Now with  $L = 230mm$  and  $E = 193GPa$  the stiffness becomes  $k = 388.2N/m$ . With equation 4.22 the eigenfrequency can be calculated.  $f_n = 57Hz$ . Now assuming that the vibration is a pure sine wave then the acceleration is given by equation 4.29 from this the maximal acceleration is given by 4.30 with  $a$  the amplitude of the sine wave ( $1mm$ ). The maximal acceleration now becomes  $\ddot{x}_{max} = 128m/s^2$ .

$$\ddot{x}(t) = -a(2\pi f_n)^2 \sin 2\pi f_n t \quad (4.29)$$

$$\ddot{x}_{max} = a(2\pi f_n)^2 \quad (4.30)$$

Since the force is given by 4.31 with the mass of the mirror arm about  $1g$ ,  $F_{max}$  becomes  $0.13N$  For safety the pretension force of the mirror arm has to be larger and is chosen to be  $1N$

$$F = ma \quad (4.31)$$

As a pretension spring a torsion spring is used. In figure 4.24 a schematic torsion spring in the pretensioned state is shown. A torsion spring cannot be twisted unlimited therefore the choice is made to use a torsion spring which legs are in an angle  $\alpha_{torsion}$  of about  $90^\circ$  in the untwisted state. The torsion spring should delivering pretension enough force when the angle  $\alpha_{torsion}$  is about  $60^\circ$  this leaves a pretension angle of  $\alpha_{twist} = 30^\circ$  of twist to generate enough pretension force.

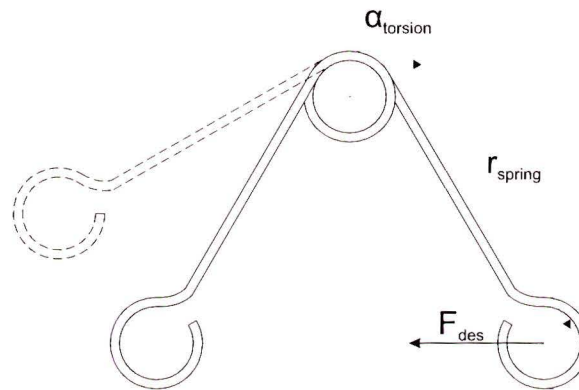


**Figure 4.24:** Schematic representation of a torsion spring

The dimensions of the spring comes from the distance between the mounting points of the spring assuming that  $\alpha_{torsion} = 60^\circ$  in the pretensioned state. The desired stiffness  $c_{des}$  is given by equations 4.32 and 4.33. Where  $F_{des} = 1N$  is the previous calculated pretension force and  $r_{spring} = 1.6mm$ . From this equation follows  $c_{des} = 4.62 \cdot 10^{-5} Nm/o$ .

The torsion spring is mounted on two pins as can be seen in 4.19. The spring is wrapped around the two pins because of the rule thats in [8]. This rules states that the the body which is not rotating relative to the force vector should mantle the body which is rotating relative to the force vector.

$$c_{des} = \frac{M_{des}}{\alpha_{twist}} \quad (4.32)$$

$$M_{des} = r_{spring} \sin \alpha_{torsion} F_{des} \quad (4.33)$$

The stiffness of a torsion spring is given by equation 4.34 [14].

$$c_{torsion} = \frac{\pi d^4 E}{11520 d_m n_w} \quad (4.34)$$

The following parameters give  $c_{torsion} = 4.64 \cdot 10^{-5}$ ,  $d = 0.16mm$ ,  $E = 190GPa$  stainless spring steel,  $D_m = 0.55mm$  and  $n_w = 1.3$ . So with a spring with these parameters the desired pretension force can be generated.

For proper functioning of the tool the Hertzian contact stress of the contact points should not exceed the maximum allowable Hertzian contact stress. When the Hertzian contact stress exceeds a maximum deformation will appear at those contacts. To calculate the Hertzian contact stress first the normal forces of the contact points should be calculated. This is done with figure 4.25 where the mirror arm and the force acting on it are represented as a freebody diagram. In this figure the contact surfaces of the v-block and with the actuation wedge are shown in red. For each contact the normal force  $F_n$ , the friction force  $F_f$  and the pretension force  $F_p$  is drawn. Also the distances (a,b,c,d) of the forces with respect to pivot point A. The force equilibrium is given by equations 4.35, 4.36, 4.37 and 4.38.

$$\sum F_x = F_{N1} - F_{f2} + F_{N3} \sin \alpha_{F3} + F_{f3} \cos \alpha_{F3} + F_v \cos \alpha_v = 0 \quad (4.35)$$

$$\sum F_y = F_{f1} + F_{N2} + F_{N3} \cos \alpha_{F3} + F_{f3} \sin \alpha_{F3} - F_v \sin \alpha_v = 0 \quad (4.36)$$

$$\sum M_A = a F_{f1} + a F_{f1} - b F_{f3} - c F_{N2} + d F_v = 0 \quad (4.37)$$

$$F_f = \mu F_n \quad (4.38)$$

The following parameter apply for this design,  $\mu = 0.15$  (stainless steel contact),  $F_v = 1N$ ,  $\alpha_v = 51.1^\circ$ ,  $\alpha_{F3} = 20^\circ$ ,  $a = 0.5mm$ ,  $b = 3.85mm$ ,  $c = 5.76mm$  and  $d = 1.96mm$ . From the force equilibrium and the parameters the following values for  $F_{N1}$ ,  $F_{N2}$  and  $F_{N3}$  are obtained,  $F_{N1} = -0.16N$ ,  $F_{N2} = 1.05N$  and  $F_{N3} = -0.31N$ .

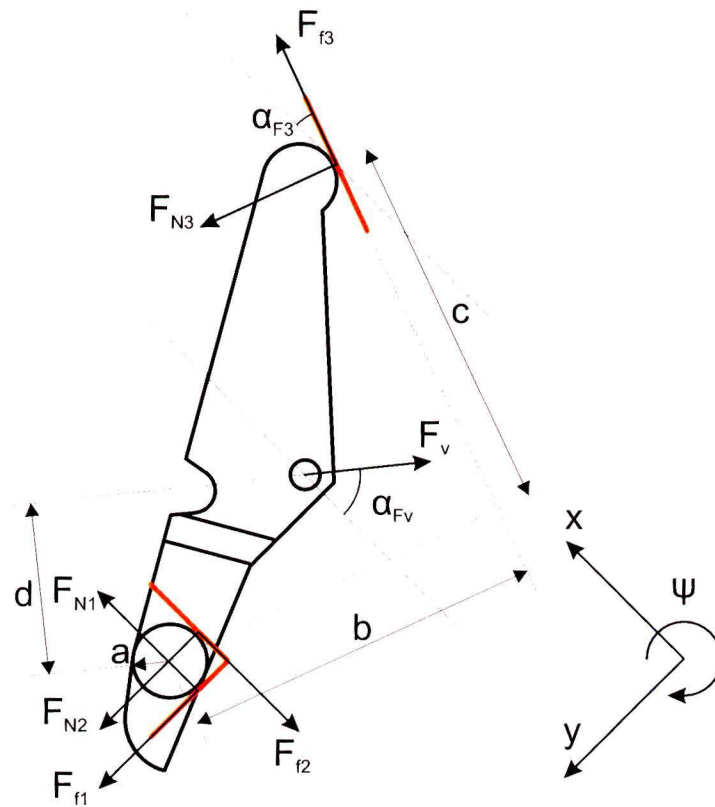


Figure 4.25: Free body diagram of the mirror arm with the forces acting on it

Now with equation 4.39 [8] the Hertzian contact stress for a line contact can be calculated.

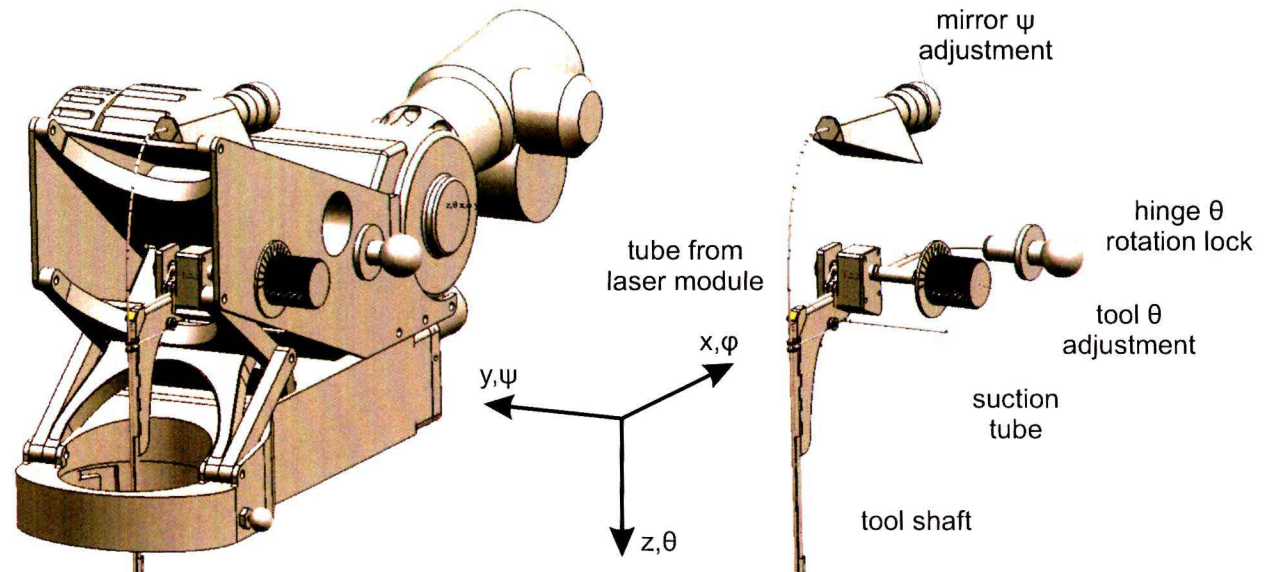
$$\sigma_{Hz} = 190 \sqrt{\frac{F}{lr}} \quad (4.39)$$

The following parameters apply, for contact 1 and 2 the same parameters apply  $r_1 = r_2 = 0.5mm$  and  $l_1 = l_2 = 0.5 \cdot 2mm$  this dimension is  $0.5 \cdot 2mm$  because there are two v-block on each side of the mirror arm, for contact 3  $r_3 = 0.5mm$  and  $l_3 = 1.6mm$ . With these parameters the following Hertzian contact stresses are calculated.  $\sigma_{Hz1} = 110N/mm^2$ ,  $\sigma_{Hz2} = 275N/mm^2$  and  $\sigma_{Hz3} = 118N/mm^2$ . These values stay well within the maximum allowable contact stress for a hardened steel contact of  $\sigma_{Hz} = 3000N/mm^2$  [8]. So when the mirror arm and v-block and the actuation wedge are hardened the contact points will not give any problems.

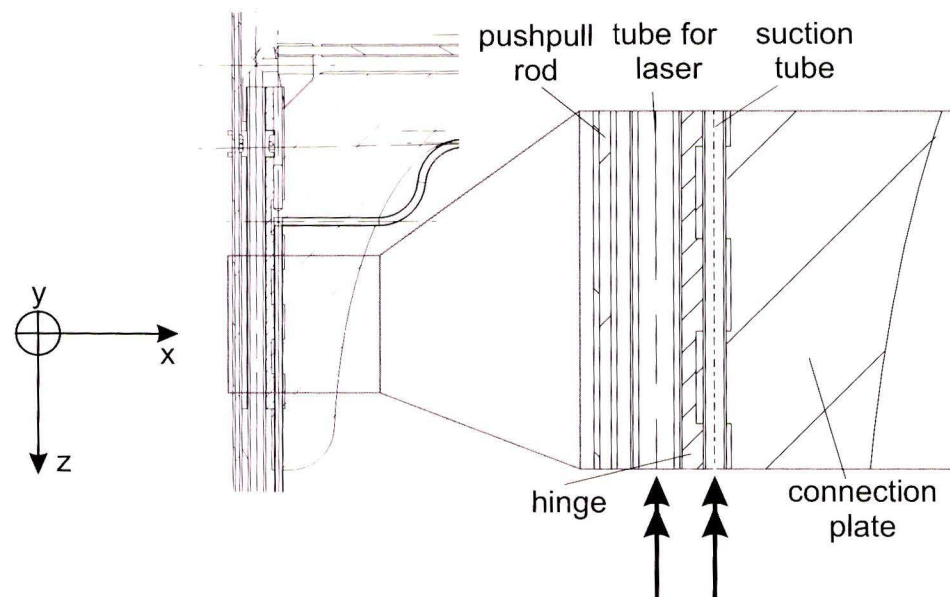
#### 4.4.3 Actuation

The cutting tool needs three directions actuated, the  $\theta$  of the cutting tool to cut around the tumor, the  $\theta$  of the hinge to rotate the tool away for aiming the suction tube and the  $\psi$  of the mirror arm to move the laser bundle from, to and underneath the tumor.

Figure 4.26 shows the part of the tool that is outside the laryngoscope. The tube coming from the laser module is connected to the suction tube with a plate. This connection plate connects the laser tool to the z-manipulator. Figure 4.27 shows how the rotations are implemented in the connection plate.



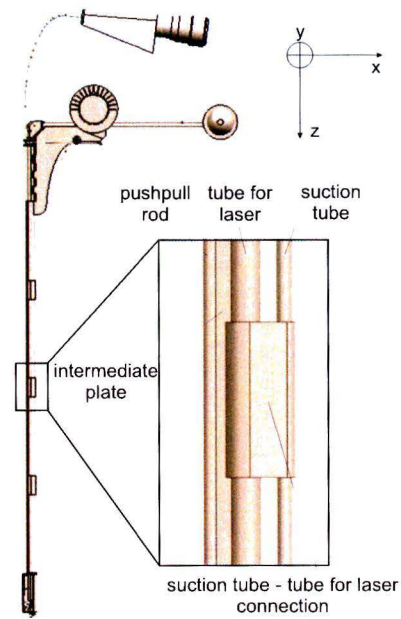
**Figure 4.26:** Part of the laser cutting tool that is outside of the laryngoscope.



**Figure 4.27:** Cross-section of the hinge implemented in the connection plate to show the rotations possible

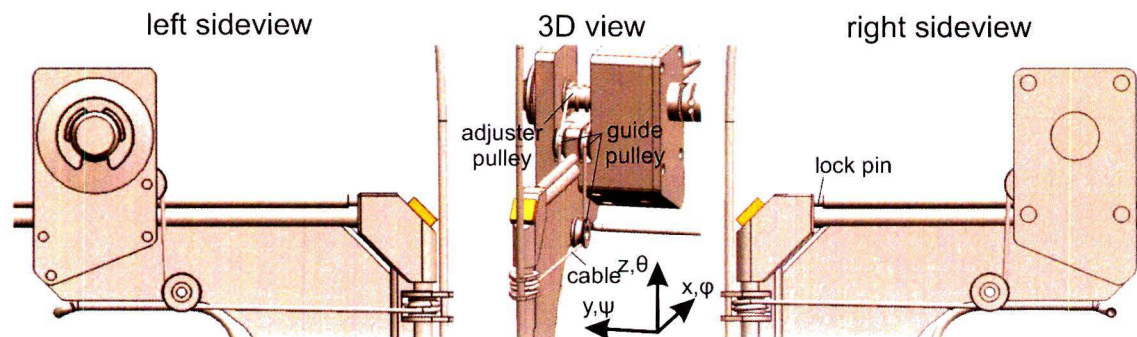
The rotation around the suction tube is achieved with a hinge type of structure. One half of the hinge is incorporated in the connection plate and the other half is connected to the tube for the laser, the suction tube is used as the shaft of the hinge. The tube for the laser can rotate in  $\theta$  in the half of the hinge it is fixed to.

Figure 4.28 shows a part of the tools shaft which is going down the laryngoscope. Along this shaft three of this kind of connections are placed to keep the tube for the laser and the tube for the vacuum together. Both tubes can rotate free in these connections. The pushpull rod is fixed to the tube for the laser with an intermediate plate. This part glues or solders the push pullrod and the tube for the laser together. This is possible because the pushpull rod has to follow the rotation of the tube for the laser but does not rotate around its own centerline.



**Figure 4.28:** Tool shaft interconnections between the tube for the vacuum, the tube for the laser and the pushpull rod

The  $\theta$  of the tool is adjusted with a cable as shown in figure 4.29. The cable is wrapped around a pulley on the tube for the laser and via some guide pulleys to the adjuster pulley. The cable is pretensioned with a spring that is put between the ends of the cable. The adjuster pulley has the same radius as the pulley on the tube for the laser. Therefore the transmission ratio is one such that the rotation of the tube for the laser equals the rotation of the adjuster pulley. The  $\theta$  adjustment of the tool is made discrete. So the arc around the tumor is cut in steps at each step the  $\theta$  rotation of the tool is locked and a shot with the laser can be fired.



**Figure 4.29:** Cable actuation of the  $\theta$  of the laser tube and the  $\theta$  of the tube for the vacuum

To determine the number of increments needed for the tool the minimum number of increments that are needed to cut the arc with the largest radius possible should be calculated. Figure 4.30 shows a part of the arc with the largest radius ( $r_{max}$ ) and the red line as the laser bundle with  $W_{max}$  as the maximum width.  $\beta_{max}$  gives the angle of the arc which is covered by the laser cut. Equation 4.40 shows how  $\beta_{max}$  is calculated and 4.41 calculates the number of increments  $n_{incr}$  needed to cut the arc with an angle of  $180^\circ$ . In this design  $W_{max} = 1mm$  and  $r_{max} = 3mm$ , now  $\beta_{max} = 18.9^\circ$  and with that  $n_{incr} = 10$ . With this number of increments there is no overlap between the cuts, to be sure that the arc is cut right some overlap between the laser shots is needed. Therefore the number of increments is chosen to be 14.

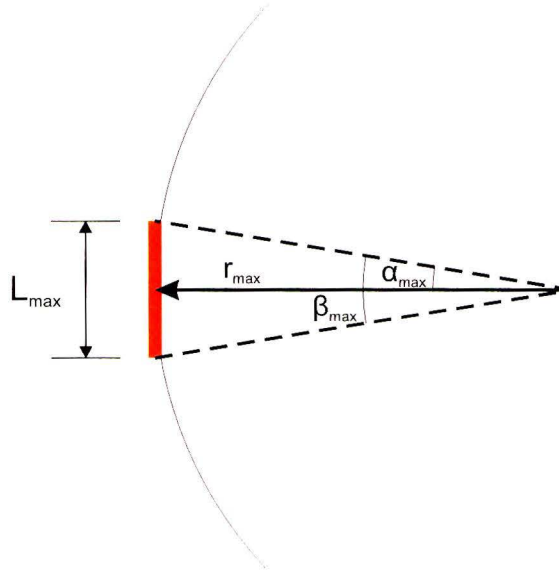


**Figure 4.30:** Angle of the arc to be cut with the largest radius possible covered but one laser cut with the maximum width

$$\beta_{max} = 2 \tan \left( \frac{W_{max}}{2r_{max}} \right) \quad (4.40)$$

$$n_{incr} = \frac{180}{\beta_{max}} \quad (4.41)$$

The discrete adjustment is implemented in the design as shown in figure 4.31. A gear is put on the shaft of the adjuster pulley. The gear in this figure has 28 teeth to achieve the 14 increments in  $180^\circ$ . A lock pin is pushed into the gear by a spring. This pin locks the gear in place. When the knob is rotated the lock pin is pushed down by the gear and is then pushed in between the next two teeth. The knob to adjust the  $\theta$  of the tool tip is on the side of the z-manipulator laser connection tube. There is also a ring placed which indicates in which increment the tool is. The lock pin is fitted in a hole. Around the lock pin two rubber rings are placed. These rubber rings pretension the pin in the hole such that there is no play between the lock pin and the whole.

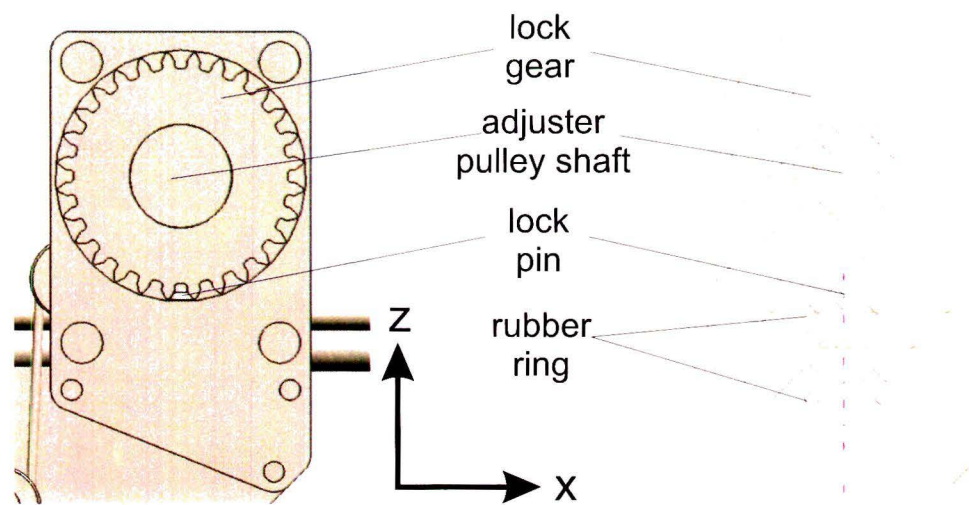


**Figure 4.31:** Increment/lock mechanism for the  $\theta$  for the laser tube

The  $\theta$  of the hinge is also adjusted with the adjuster pulley. The  $\theta$  rotation of the hinge is locked with a pin when this pin is retracted this rotation is unlocked. This pin is shown in figure 4.29. This pin can be retracted with the knob on the side of the laser connection tube. The tip of the pin and the hole in which the pin sits are slightly conical. when the pin is pushed in the hole it will center and push out the play.

The angle of the mirror arm and thus the distance from the tumor to the laser beam is adjusted with the wedge discussed in the previous section. The wedge is actuated with a microscrew that is connected to the wedge via a pushpull rod. This pushpull rod runs parallel to the tube for the laser and is fixed to the microscrew which is placed on top of the laser connection tube. Figure 4.32 shows the cross-section of the microscrew module. This figure shows that the pushpull rod is pushed against the microscrew by a spring. This spring is providing pretension on the pushpull rod and the microscrew such that the pushpull rod will follow the motion of the microscrew.

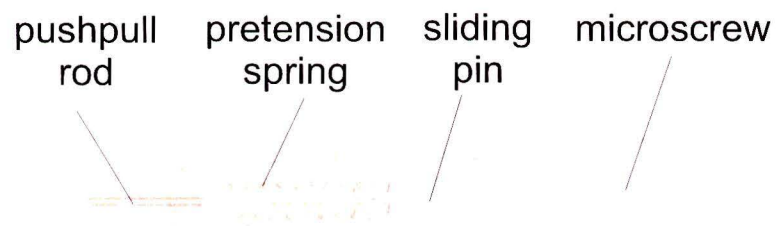


**Figure 4.32:** Pretensioning of the pushpull rod against the microscrew





## Chapter 5

### Conclusion

Laryngeal surgery (removing tumors from the vocal folds) is done minimally invasive as much as possible. This means that a tube called a laryngoscope is inserted into the mouth of the patient to the larynx. This gives better access to the larynx via the mouth, because the laryngoscope is lining the mouth, throat and larynx up. By using the laryngoscope no incisions are needed to reach the operation field therefore outside scarring and recovery time is reduced. The laryngoscope is also the limiting factor with this kind of surgery. Because the laryngoscope is a tube which is limiting all DOF's except  $z$  and  $\theta$  (figure 4.1). Tumors are often cut from the vocal fold using a laser (AcuPulse™) and attachment for laryngeal surgery (AcuBlade™). The limitations on this laser caused by the laryngoscope result in that instead of aiming the laser at the point that has to be cut, the point to be cut must be manipulated such that the laser beam is aimed at it. For the manipulation currently forceps are used but they have a long thin shaft because they have to reach through the entire length of the laryngoscope. This long shaft results in amplification of the tremor of the hands of the surgeon.

For these problems a new laser tool is designed. This laser uses mirrors to guide the laser beam. Using these mirrors makes it possible to not only cut along the laryngoscope but also at an angle with respect to the centerline of the laryngoscope. The angle with respect to the centerline of the laryngoscope that can be reached with the tool is  $30^\circ$ . This cutting at an angle makes it possible to cut underneath the tumor. Cutting underneath the tumor results in more healthy tissue under the tumor can be left behind. Leaving more healthy tissue behind reduces the risk of complications such as loss or change of voice. To keep the tumor in place during cutting with the laser a vacuum line is used. The vacuum line is connected to the laser cutter. When the tumor is grabbed with the vacuum line the tumor has a fixed position with respect of the tool. The laser can cut in an arc of  $200^\circ$  around the vacuum line. When the tumor is cut loose the vacuum line can be used to remove the tumor out of the larynx via the laryngoscope.

To position the vacuum line onto the tumor an  $x,y,\theta$ -manipulator and a  $z$ -manipulator are designed. The  $z$ -manipulator is used to lower the tool tip which is containing the mirrors to guide the laser beam and suction tube onto the tumor. The range of this  $z$ -manipulator is  $10\text{mm}$  this is sufficient to retract the tool enough to see the tumor past the vacuum line and to compensate for deviation in the positioning of the laryngoscope in the throat of the patient. The  $z$ -manipulator is driven by an electro motor. This electro motor achieves a  $z$ -speed of  $1\text{mm/s}$

The ranges of the  $x,y,\theta$  manipulator come from the dimensions of the standard laryngoscope (figure 2.5) which has a circular opening of  $13\text{mm}$  in diameter. Therefore the  $x,y,\theta$ -manipulator is designed such that the  $x$  and  $y$  range is  $13\text{mm}$ . Which is adjusted with a micro screw with resolution  $10\mu\text{m}$ .

The theta has a range of  $180^\circ$ . This range is designed that when working on the right vocal fold the laser tool can be positioned to the left such that it is not in the view of the surgeon and the other way around. When another position of the tool is desired every position between left ( $0^\circ$ ) and right ( $180^\circ$ ) is possible.

This design also resulted in a stiffer frame for the fixation of the laryngoscope. This means that there is no need for the surgeon to fix the laryngoscope with medical tape, as shown in figure 2.4. This better fixation of the laryngoscope makes it also possible to fix the laser tool physically via the frame to the laryngoscope. Now the force loop is going from the laryngoscope via the laryngoscope arm and the support rods to the laser tool. Instead of going via the patient, operating table, floor and microscope.

There are still a couple of things that have to be done before the design is complete. First the clamping functions of the laryngoscope arm still have to be designed. So clamping the hub onto the frame tube to lock the  $x$  and  $\phi$  (figure 3.7) of the laryngoscope arm and the clamping of the laryngoscope in the laryngoscope clamp and fixing the  $\phi$  of the laryngoscope clamp. Also a clamping function on the  $x, y, \theta$  to lock those three DOF's should be designed. It can be a clamp which is clamping the flange between the top and bottom plate of the  $x, y, \theta$  manipulator (figure 4.4).

# Bibliography

- [1] R. A. Faust, *Robotics in Surgery*. New York: Nova Science Publisher, Inc, 2007.
- [2] G. Wolf-Heidegger and P. Köpf-Maier, *Wolf-Heidegger's Atlas of Human Anatomy: Head and neck, thorax, abdomen, pelvis, CNS, eye, ear*. Wolf-Heidegger's Atlas of Human Anatomy, Karger, 2005.
- [3] H. Mulder, *Keel-, Neus,- en Oorchirurgie*. Maarsen: Elsevier Gezondheidszorg, 2005.
- [4] Storz, *Extract from Catalog ENT, Laryngology*, 8th ed., 2008.
- [5] Lumenis Inc, *AcuPulse™ CO<sub>2</sub> Laser with Surgitouch™ Automation System*, 2008.
- [6] Lumenis Inc, *Digital AcuBlade™ Robotic Laser Microsurgery System*, 2005.
- [7] T. M. J. van Oekelen, "Dined antropometric database." <http://dined.io.tudelft.nl/dined/>, 2004.
- [8] P. C. J. N. Rosielle, *Constructieprincipes*. Eindhoven: TU/e, 2007.
- [9] Standa, *Microscrews 9S75M-AL*.
- [10] SKF, *Miniature Profile Rail Guides*, 2006.
- [11] Ozak, *MS series Miniature Slide Screw*.
- [12] V. B. Bhandari, *Design of Machine Elements*. New Delhi: Tata McGraw-Hill Publishing Company Limited, 2007.
- [13] Maxon, *Program 2011/12 High Precision Drives and Systems*, 2011.
- [14] "Alcomex veren b.v." [http://www.alcomex.nl/Technische\\_informatie/Technische\\_informatie\\_-7-/technische\\_informatie\\_-7-.html](http://www.alcomex.nl/Technische_informatie/Technische_informatie_-7-/technische_informatie_-7-.html).



## Appendix A

### z-Manipulator

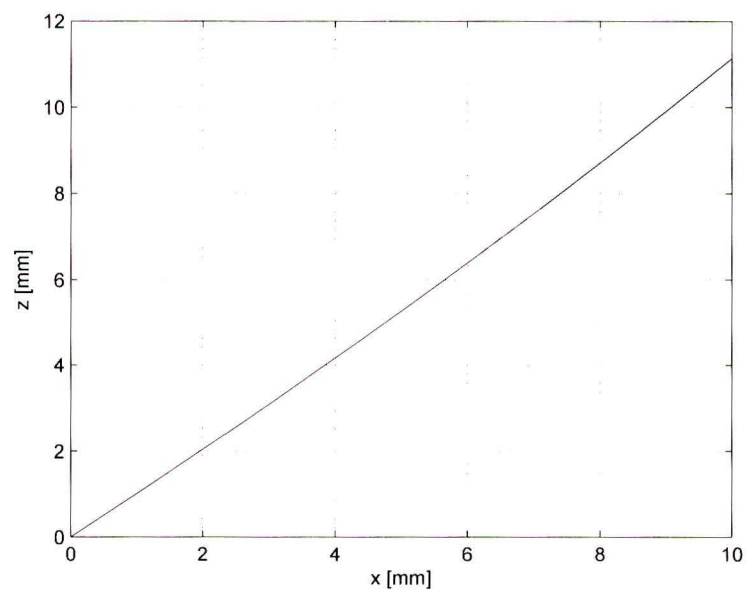


**Figure A.1:** Relation between the  $x$ -displacement of point B in [mm] and the  $z$  displacement of point D in [mm]

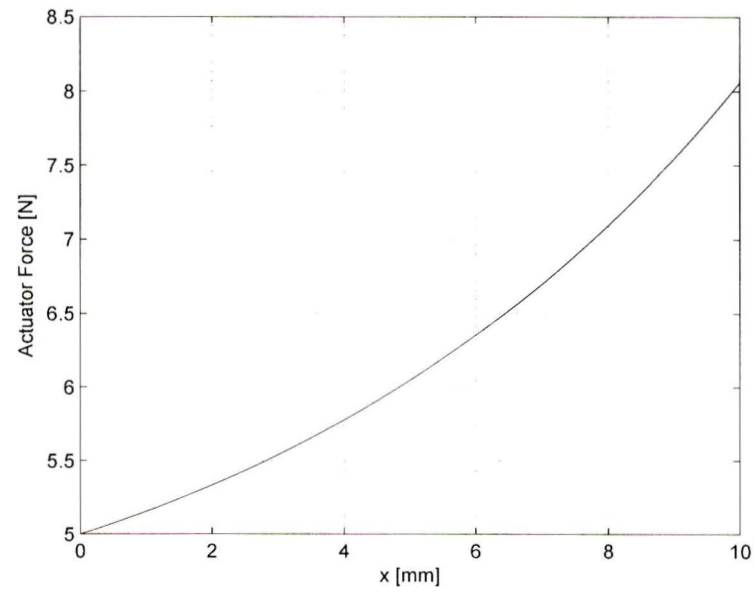


**Figure A.2:** Needed Actuator force for lifting the load in [N] against input position  $x$  in [mm]

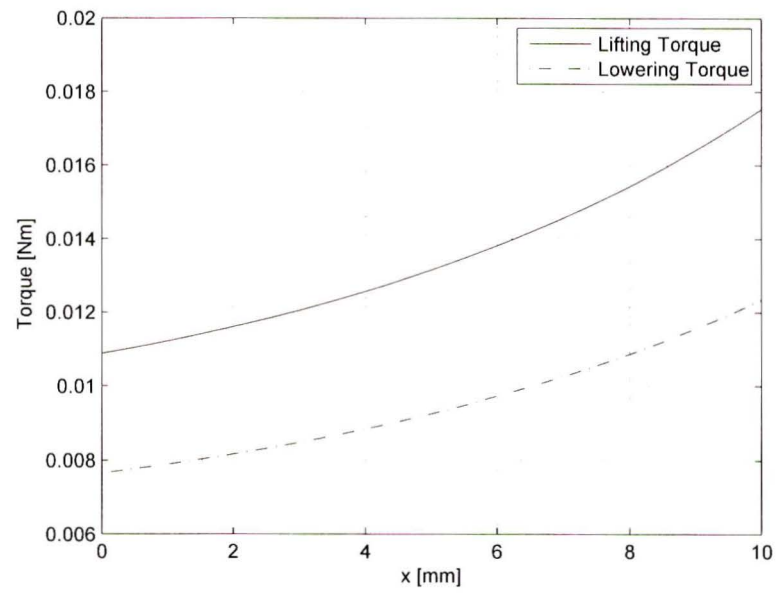


**Figure A.3:** Motor torque needed to lift or lower the load on the spindle on the  $y$ -axis and  $x$  position in [mm]

## Appendix B

### Cutting Tool

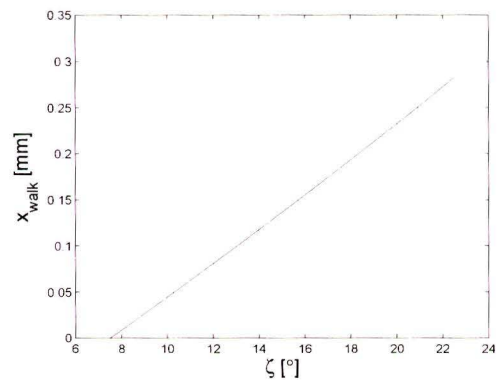


**Figure B.1:** Walk of the laser beam on the mirror in [mm] depending on the mirror angle  $\zeta$  in [ $^{\text{circ}}$ ]

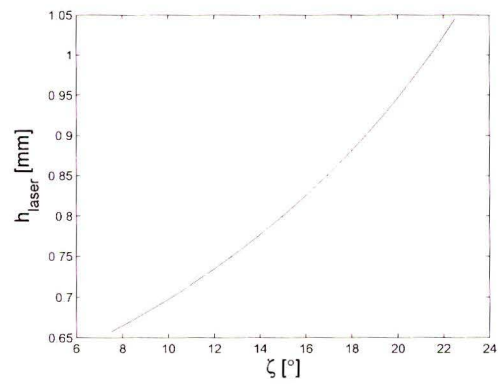


**Figure B.2:** Height of the laser beam on the mirror in [mm] depending on the mirror angle  $\zeta$  in [ $^{\text{circ}}$ ]



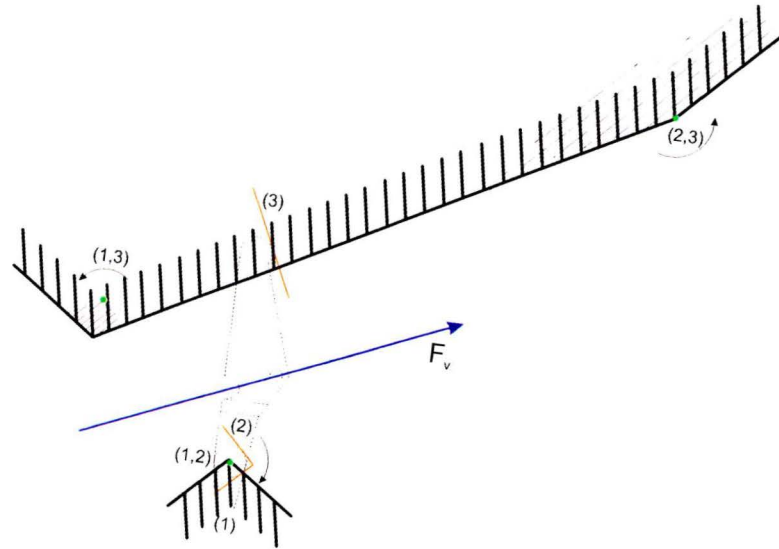


**Figure B.3:** Wittgens graphical method for the minimal ( $\zeta = 7.5^\circ$ ) mirror angle

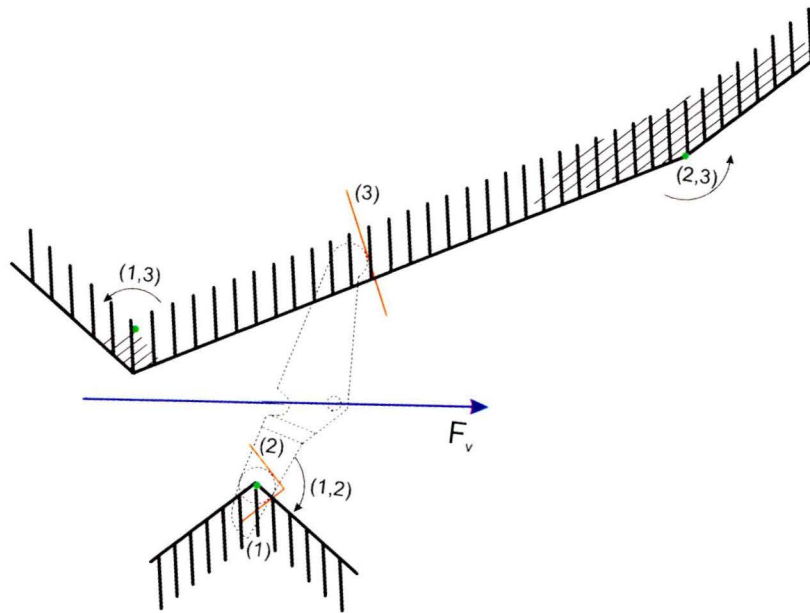


**Figure B.4:** Wittgens graphical method for the maximal ( $\zeta = 22.5^\circ$ ) mirror angle

## Appendix C

### Forceps

During this project there were also some ideas about the forceps they are shown with sketches in this appendix. As can be seen in figure 2.7 there are a lot of different forceps. The main cause for this is the limited freedom in the laryngoscope. For this reason every kind of forceps is made five times, one with a straight tip and four others with the tip bent to the left or right, up or down. This results in an instrument table full of forceps. It would be nice to reduce the number of forceps.

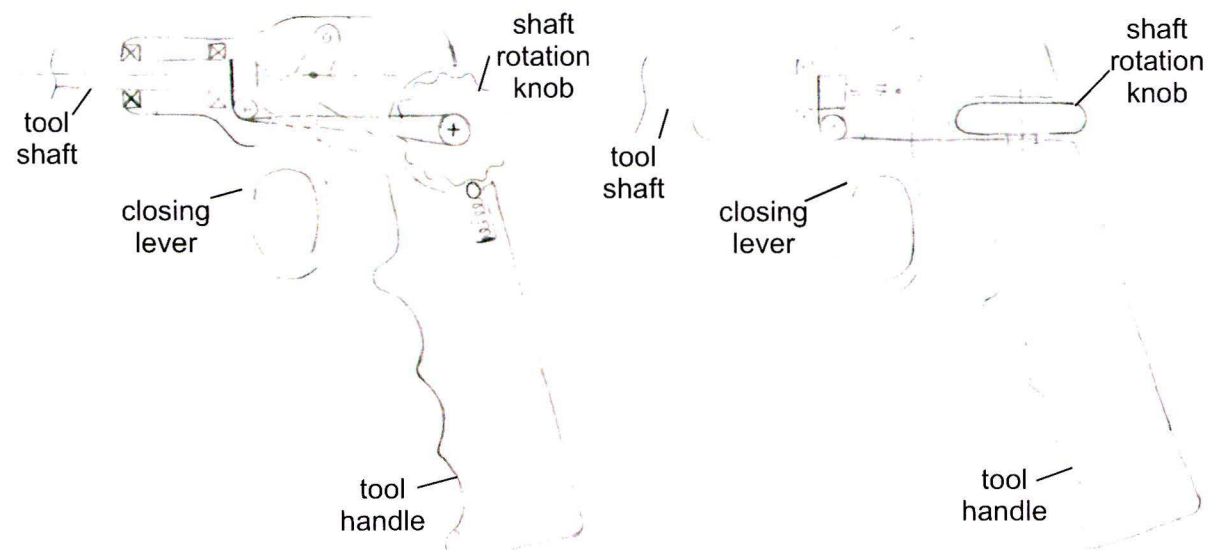
When looking at the forceps with the tip pointing up, down, left and right, these positions are rotation symmetric around the tool shaft. So when the forceps are made such the tool shaft can be rotated, these four positions can be reached. It is even possible for the tool to reach positions between the four positions given earlier, making the forceps even more versatile.

The surgeon is looking along the tool shaft when operating. Therefore the tool shaft rotation mechanism has to be compact such that it is not blocking the view of the surgeon. It should also be easy to operate the rotation of the tool shaft with the same hand as you are holding it. This makes it easy to make adjustments with the tool without removing it from the laryngoscope.

The scissor like handles of the forceps make them such that when they are not pulled together by the fingers of the surgeon they are not sitting firmly into the hands of the surgeon. Together with the long shaft between the handle and the tool tip this is making the handling of the forceps hard and inaccurate. To make sure that the forceps are firmly in the hands of the surgeon even when the forceps aren't closed a new handle is designed. In the following figures the sketches of these ideas are shown.

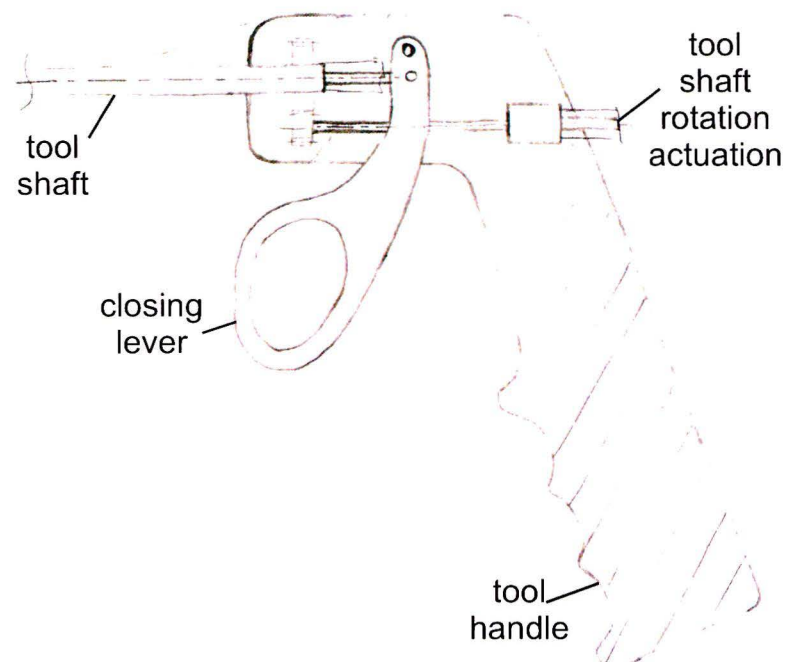
Figure C.1 shows the new handle designed. This handle sits in the palm of the hand of the surgeon with his index finger the closing lever, which is used to open and close the forceps, is operated. This handle makes the surgeon holding the tool with his whole hand and not only with two fingers as with the current forceps. When the tool is more firm in the hand of the surgeon the tool can be manipulated more precise.

This figure also shows two knobs that can be used to rotate the tool shaft. The rotation of this knob is transferred via a cable to the tool shaft. This rotation knob can easily be operated with one hand. In the left sketch the rotation knob is placed in the plane of the tool handle therefore it will not block the view of the surgeon. The sketch on the right has the knob placed perpendicular to the tool handle this appears to be less compact but because it is placed as far as possible from the tool shaft it will not block the view of the surgeon.



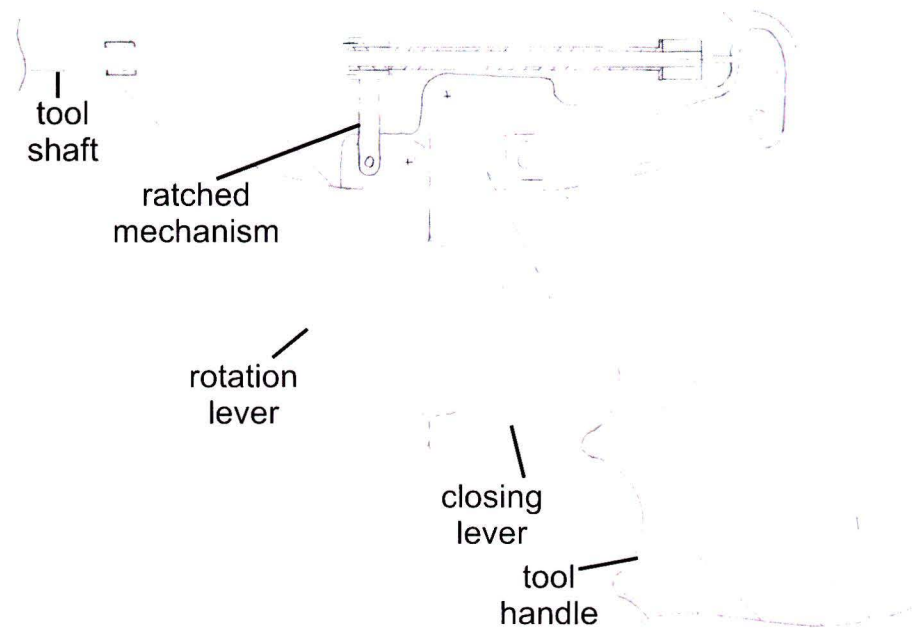
**Figure C.1:** Sketch of a tool with an improved handle and two different versions of knobs for the rotations of the tool shaft

Figure C.2 uses a click mechanism to rotate the tool shaft. The click mechanism should work like a pen mechanism. With every click the output shaft is rotated a step. This system is easy to operated with one hand and is can be really compact. The compactness depends on the chosen gears, when the gear on the tool shaft is small enough it will not block the surgeons view to much.



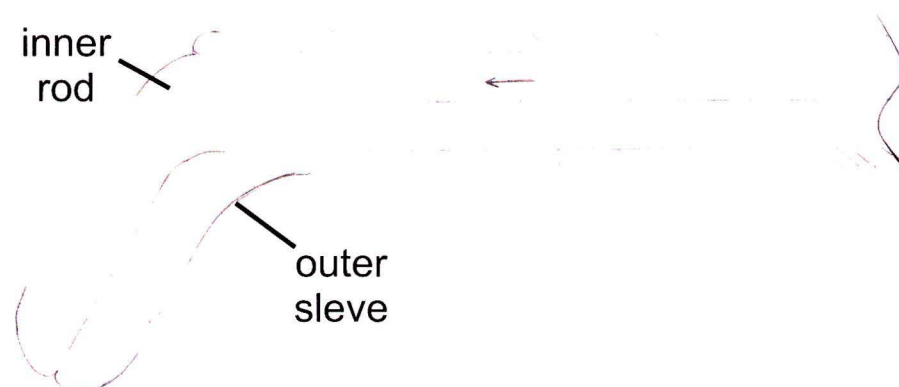
**Figure C.2:** Sketch of a tool with an improved handle with a click mechanism as an actuation unit for the rotation of the tool shaft

Figure C.3 uses a lever operated by the index finger to rotate the tool shaft. This lever is used as the lever for a ratchet mechanism. This ratchet mechanism is fitted on the tool shaft and is used to lock and rotate it. So with this design the opening and closing of the tool tip and the rotation of the tool shaft are both operated with the index finger.



**Figure C.3:** Sketch of a tool with an improved handle with a ratchet mechanism actuated by a lever to rotate the tool shaft

A new idea for a tool tip is shown in C.4. This tool tip uses the same kind of shaft as the current forceps. With an inner rod that can slide in the outer sleeve. One of the jaws is fixed to the outer sleeve and the other is fixed to the inner rod as shown in figure C.4. This sliding motion makes the tool tip open and close. The advantage of this tool tip is that the pivot point of the current tool tip is eliminated and therefore also the play in that pivot point. To this idea only a rotation lock should be added to the tool tip such that the inner rod cannot rotate with respect to the outer sleeve.



**Figure C.4:** Sketch of an idea for a new tool tip with less components and play